Bose-Einstein beams: Coherent propagation through a guide

P. Leboeuf and N. Pavloff

Laboratoire de Physique Théorique et Modèles Statistiques, Université Paris Sud, Bâtiment 100, F-91405 Orsay Cedex, France
(Received 14 March 2001; published 3 August 2001)

We compute the stationary profiles of a coherent beam of Bose-Einstein-condensed atoms propagating through a guide. Special emphasis is put on the effect of a disturbing obstacle present in the trajectory of the beam. The obstacle considered (such as a bend in the guide, or a laser field perpendicular to the beam) results in a repulsive or an attractive potential acting on the condensate. Different behaviors are observed when the beam velocity (with respect to the speed of sound), the size of the obstacle (relative to the healing length), and the intensity and sign of the potential are varied. The existence of bound states of the condensate is also considered.

I. INTRODUCTION

The field of Bose-Einstein condensation (BEC) of atomic vapors is undergoing a rapid experimental development, providing a rich new phenomenology and also allowing the testing of concepts that originated in other fields (mainly in the theory of superfluidity, in nonlinear optics, and in atomic physics). Along these lines, the possibility of building atom lasers by guiding condensed particles through various geometries opens up the prospects of a rich variety of interference, transport, and/or coherence phenomena. Cold atoms have already been propagated in various guides (see, e.g., [1–4] and references therein); more and more efficient coherent sources of atoms have recently been designed (using various output coupling schemes; see Refs. [5–9]) and continuous guided beams of condensed atoms will be accessible in the near future (see the preparatory study [10]).

The purpose of the present work is to explicitly determine the different propagating modes of a beam of condensed atoms through a guide, as a function of the various external control parameters. We consider the simplest geometry, in which a guide connects two reservoirs, and treat the case of atoms with a repulsive effective interaction, such as rubidium and sodium. First, the transmission through a straight guide is reevaluated: small amplitude density oscillations, cnoidal waves, and gray solitons are possible propagating modes. The main part of the paper is devoted to the study of coherent transmission modes in the presence of an obstacle. We find that, as a function of the speed of the incoming beam and the size and depth of the perturbing potential, many different transmission modes exist. For example, some are solitonlike modes (with a peak or a trough in the density) that are pinned to the obstacle. They may also have density oscillations in the region of the obstacle. On the contrary, other modes are steplike shaped. In general, the modes may or may not have a wake. The wake, however, always precedes the obstacle (it never occurs downstream).

The obstacle is represented in our treatment by a potential that acts on the condensate along the axis of the guide. It can be repulsive or attractive. There are at least two simple ways

to realize such an obstacle experimentally. The first is to bend the guide: a potential proportional to the square of the local curvature is created. This potential is always attractive. In view of future applications of the atom laser to more complicated geometries, the presence of bends seems unavoidable and their study is therefore far from academic. The second possibility is to illuminate the beam with a detuned laser field. Contrary to the case of a bend, attractive and repulsive potentials may be realized by varying the frequency of the laser. This latter method also has the advantage of allowing a better control of the relative speed between the obstacle and the beam (if using an acousto-optic deflector).

In the case of attractive potentials, aside from the transmission modes there may also exist bound states in the guide, in which condensed atoms are trapped without possibility of escape. These bound states are also analyzed here. In the case of a bend we show that, due to the intra-atomic interactions, the bound state can support only a limited number of condensed atoms, which is typically of the order of 100 for rubidium and sodium. However, this number can be made much larger for an attractive potential originating from a red detuned laser field.

The paper is organized as follows. In Sec. II we set up the theoretical framework and notation. Our approach for describing the condensate motion is based on a one-dimensional (1D) reduction of the Gross-Pitaevskii equation [11]. The solutions described here can in some instances be explicitly written in an analytic form, for example, in terms of elliptic functions. Although we use this opportunity in some cases, we have chosen to keep the discussion at a qualitative level. This allows us to cover a large range of experimental situations and gives a global view of all the possible solutions in the different regimes of the control parameters. In Sec. III we study the existence of a bound state of the condensate created by an attractive potential. We determine the maximum number of atoms the bound state can accommodate. In Secs. IV–VII we study the propagation of a condensate through a guide connecting two reservoirs. The analysis relies on an interpretation of the Gross-Pitaevskii equation in terms of a fictitious classical dynamics. We focus on different specific examples, starting with a straight waveguide without any potential (Sec. IV). We then study the motion in the presence of an obstacle represented by an attractive (Sec. V) and a repulsive (Sec. VI) square well. Sec-

---

tion VII presents two alternative treatments for determining the transmission modes in the presence of an obstacle. The first one is a perturbative approach; the second approximates the external potential by a δ function. Section VIII contains an analysis of the results in view of future experimental realizations. We present our conclusions in Sec. IX. Some technical aspects concerning the adiabatic approximation used for deriving the 1D reduction of the Gross-Pitaevskii equation are included in the Appendix.

II. AN EFFECTIVE ONE-DIMENSIONAL EQUATION

We consider BEC atoms at zero temperature confined to a waveguide. Let x be the coordinate along the axis of the guide (which is possibly bent) and $\vec{r}_\perp$ a perpendicular vector giving the transverse coordinates. We work in the adiabatic regime where the local curvature $\kappa(x)$ of the longitudinal motion of the atoms is small. If the transverse extension of the wave function is denoted by $R_\perp$, this is more precisely defined by the limit $R_\perp \kappa \ll 1$ and $|d\kappa/dx| \ll 1$ (see the Appendix). In this regime one can consider x and $\vec{r}_\perp$ as Cartesian coordinates, for instance, the volume element d^3r is approximately $dx\,d^2r_\perp$.

It is consistent with the adiabatic approximation to make an ansatz for the condensate wave function $\Psi(\vec{r},t)$ of the form [11]

$$\Psi(\vec{r},t)=\psi(x,t)\phi(\vec{r}_\perp;n) \tag{1}$$

where ϕ is the equilibrium wave function for the transverse motion, normalized to unity, $\int d^2r_\perp|\phi|^2=1$. $\psi(x,t)$ describes the longitudinal motion, and the density per unit of longitudinal length is

$$n(x,t)=\int d^2r_\perp|\Psi|^2=|\psi(x,t)|^2. $$

Notice that the transverse wave function depends parametrically on $n(x,t)$. The adiabatic approximation is in fact a local density approximation in the sense that one assumes that the transverse motion is not affected by densities at points other than x. As noted in Ref. [11] this corresponds to the assumption that the transverse scale of variation of the profile is much smaller than the longitudinal one (and corresponds indeed to the limit $R_\perp \kappa \ll 1$).

The beam is confined by a transverse potential $V_\perp(\vec{r}_\perp)$. Keeping in mind experimental realizations, we often consider below the particular case of a harmonic trapping $V_\perp(\vec{r}_\perp)=\frac{1}{2}\omega_\perp^2 r_\perp^2$ ($\omega_\perp$ is the pulsation of the harmonic oscillator; we set units such that $\hbar=m=1$). As shown in the Appendix, within the adiabatic approximation the presence of a bend results in an attractive longitudinal potential $V_\parallel(x)$ given by

$$V_\parallel(x)=-\kappa^2(x)/8. \tag{2}$$

The Gross-Pitaevskii equations for the condensate are derived through a variational principle. One extremizes the action

$$S=\frac{i}{2}\int d^3r\,dt(\Psi^*\partial_t\Psi-\Psi\partial_t\Psi^*)-\int dt\,\mathcal{E}[\Psi], \tag{3}$$

where $\mathcal{E}[\Psi]$ is the energy functional

$$\mathcal{E}[\Psi]=\int d^3r\left(\frac{1}{2}|\vec{\nabla}\Psi|^2+2\pi a_{sc}|\Psi|^4+(V_\parallel+V_\perp)|\Psi|^2\right). \tag{4}$$

a_{sc} is the s-wave scattering length of the interatomic potential (which is represented by a δ function interaction). In all the present work, we consider the case of repulsive interatomic interactions, $a_{sc}>0$. The extremization of S with Lagrange multiplier $\epsilon(n)$ imposing the normalization $\int d^2r_\perp|\Psi|^2=n$ for each x (more precisely for each n) leads to the following equations [11]:

$$-\frac{1}{2}\vec{\nabla}_\perp^2\phi+(V_\perp+4\pi a_{sc}n|\phi|^2)\phi=\epsilon(n)\phi \tag{5}$$

and

$$-\frac{1}{2}\partial_{xx}^2\psi+(V_\parallel+\epsilon(n))\psi=i\partial_t\psi. \tag{6}$$

In Eq. (6) the nonlinear term $\epsilon(n)$ (remember that $n=|\psi|^2$) is determined as a function of n from Eq. (5). In the low-density limit $a_{sc}n\ll 1$ the nonlinearity in Eq. (5) is small. In this case, a perturbative solution of Eq. (5) leads to

$$\epsilon(n)=\epsilon_0+2a_{sc}n/a_\perp^2, \tag{7}$$

where ϵ_0 is the eigenenergy of the ground state ϕ_0 of the transverse unperturbed Hamiltonian $-\frac{1}{2}\vec{\nabla}_\perp^2+V_\perp$, and $a_\perp^{-2}=2\pi\int|\phi_0|^4d^2r_\perp$. For a harmonic confining potential $a_\perp=\omega_\perp^{-1/2}$ is known as the oscillator length.

In the opposite large-density limit $na_{sc}\gg 1$ the Thomas-Fermi approximation holds, namely, the kinetic term in Eq. (5) can be neglected. ϵ is obtained as a function of n through the relation $N_{TF}(\epsilon)=2a_{sc}n$, where N_{TF} is the integrated Thomas-Fermi density of states $N_{TF}(\epsilon)=\int(\epsilon-V_\perp)\Theta(\epsilon-V_\perp)d^2r_\perp/(2\pi)$. For a harmonic confining potential this reads

$$\epsilon(n)=2\omega_\perp\sqrt{na_{sc}}+\epsilon_0. \tag{8}$$

We remark here that the Gross-Pitaevskii equation is valid in the dilute gas approximation, when the 3D density n_{3D} of the gas satisfies $n_{3D}a_{sc}^3\ll 1$ [12]. This reads here $na_{sc}\ll(a_\perp/a_{sc})^{2/\nu}$ ($\nu=1$ in the dilute regime and $\nu=1/2$ for high densities). $a_\perp/a_{sc}$ being typically of order 10^3, this condition will be considered as always fulfilled, even at high longitudinal densities, when $na_{sc}\gg 1$.

On the other hand, the weakly interacting 1D Bose gas picture also breaks down at very low densities, in the Tonks gas regime (recent references relevant to this discussion are [13–16]). This occurs in the regime $na_{sc}\ll(a_{sc}/a_\perp)^2\sim 10^{-6}$, which we thus discard from the present study.

Equation (6), together with Eqs. (7) and (8), are the main results of this section. They provide an effective one-dimensional equation for the description of the dynamics of the condensate along the guide. Notice that in general the nonlinear term in Eq. (6) does not have the standard cubic form of the one-dimensional Gross-Pitaevskii equation. This happens only in the low-density regime $a_{sc}n \ll 1$ when the nonlinear potential (7) is proportional to $|\psi|^2$.

We emphasize that Eq. (6) relies on an adiabatic approximation. It is well known that in many instances this approximation gives accurate results well beyond its strict domain of validity. Two examples relevant in the present context are Refs. [17] and [18], where the propagation of waves (without nonlinear effects) was studied in the extreme nonadiabatic case of waveguides with a discontinuous curvature and a sudden constriction, respectively. The adiabatic approximation was nevertheless shown to be applicable in these systems. On the basis of these examples (and of others), one can consider that the results presented here have a wide range of validity.

For practical purposes it will appear useful in the following to introduce a longitudinal healing length ξ defined for a constant longitudinal density n as

$$\frac{1}{2\xi^2} = \epsilon(n) - \epsilon_0. \tag{9}$$

This gives $\xi = \frac{1}{2}a_\perp (na_{sc})^{-1/2}$ in the low-density regime and $\xi = \frac{1}{2}a_\perp (na_{sc})^{-1/4}$ for high densities in a harmonic confining potential.

We now study in detail the different solutions of Eq. (6). Although the attractive potential $V_\parallel(x)$ appearing in the equation of motion was due to the presence of a bend in the guide, our results are very general and $V_\parallel(x)$ could be of a completely different physical origin. In particular, we will consider in Sec. VI the case of a *repulsive* potential, which cannot be produced by a bend.

III. BOUND STATES

We first study the existence of bound states in the guide due to an attractive potential $V_\parallel(x)$. The existence of bound states in the quantum mechanical motion of noninteracting particles in a bent waveguide has been extensively considered in the past (see, e.g., [19–21] and references therein). It has been shown by Goldstone and Jaffe that at least one bound state exists in two- and three-dimensional bent tubes [19] (cf. the discussion in the Appendix). The particle is trapped because its energy is lower than the first propagating mode of the straight guide. In the case of a condensed beam, we are interested in whether bound states occur in the presence of interactions.

In the extreme dilute limit $a_{sc}n \to 0$ Eq. (6) reduces to an ordinary one-dimensional Schrödinger equation and the existence of a bound state in $V_\parallel(x)$ is guaranteed by general theorems of quantum mechanics [22]. Hence there exists a state of the condensate whose energy is lower than the energy ϵ_0 of the first propagating mode of the guide. This state is localized in the region where $V_\parallel$ is noticeable, and we

assume for simplicity that this happens in some finite region around $x=0$. With increasing number of atoms in the condensate the nonlinear effects come into play. The repulsive intra-atomic interaction increases the energy of the bound state (as well as its spatial extension), and there is a threshold beyond which this state disappears. Therefore for a sufficiently large number of atoms no bound state is expected to occur. We now determine the threshold quantitatively by determining the maximum number of Bose-Einstein-condensed atoms the bound state can accommodate.

Near the threshold the state is very weakly bound, and the wave function extends over distances much greater than the range of the potential $V_\parallel$. Hence, in this limit it is legitimate to make the approximation $V_\parallel(x) \approx \lambda\,\delta(x)$, with $\lambda = \int_{-\infty}^{+\infty} V_\parallel(x)dx < 0$. This approximation is not contradictory with the assumption of adiabaticity of the motion.

We look at stationary solutions of Eq. (6) of the form $\psi(x,t)=A(x)\exp(-i\mu t)$, μ being the chemical potential and A a real function. In the regions where the potential is negligible (i.e. for $x \neq 0$ with the above replacement of $V_\parallel$ by a δ function) Eq. (6) can be integrated once, giving an equation for $n(x) = A^2$:

$$-\frac{n'^2}{8n} + \varepsilon(n) = \mu n \quad \text{where} \quad \varepsilon(n) = \int_0^n \epsilon(\rho)d\rho. \tag{10}$$

With the convention defined in Sec. II, the normalization is $\int_{-\infty}^{+\infty} n(x)dx = N$, where N is the total number of particles in the bound state. The density n can be shown to be an even function of x, and the matching condition at $x=0$ reads $n'(0^+) = 2\lambda n(0)$ (the prime denotes d/dx). Using Eq. (10) and these two conditions we arrive at a set of two equations determining $n(0)$ and μ as functions of λ and N,

$$\frac{\lambda^2}{2}n(0) = \varepsilon(n(0)) - \mu n(0) \tag{11}$$

and

$$\int_0^{n(0)} \frac{(n/2)^{1/2}dn}{\sqrt{\varepsilon(n)-\mu n}} = N. \tag{12}$$

For solving this system, one needs to know the explicit form of the function $\varepsilon(n)$. We will see that for realistic values of λ corresponding to an attraction issued from a bend in the guide the bound state can accommodate only a small number of particles. In the case of a bend, it is thus sensible to concentrate on the low-density limit (see the estimate at the end of this section). Using Eq. (7), in the low-density regime we have $\varepsilon(n) = \epsilon_0 n + a_{sc} n^2/a_\perp^2$ and we obtain

$$\mu = \epsilon_0 - \frac{1}{2}\left(\int_{-\infty}^{+\infty} V_\parallel(x)dx + \frac{a_{sc}}{a_\perp^2}N \right)^2. \tag{13}$$

The first, negative, term inside the large parentheses is due to the attractive potential produced by the bend [cf. Eq. (2)], while the second one comes from intra-atomic repulsive interactions in the condensate. Equation (13) clearly displays

the existence of a threshold. When the number of atoms N occupying the bound state increases, the chemical potential μ increases and eventually reaches the threshold ϵ_0 at which the state disappears. This occurs for a number of atoms N_{max} given by

$$N_{max} = \frac{a_\perp^2}{a_{sc}} \left| \int_{-\infty}^{+\infty} V_\parallel(x) dx \right|. \qquad (14)$$

For an arbitrary potential, as $N \to N_{max}$ the spatial extension of the bound state diverges. Thus the approximation of $V_\parallel$ by a δ-function is well justified in that limit, and we expect Eq. (14) to be very accurate [23].

The order of magnitude of N_{max} can be estimated by considering a bend of constant radius of curvature R_c and bending angle θ. From Eqs. (2) and (14) we get $N_{max} = a_\perp^2 \theta/(8 a_{sc} R_c)$. For a guide with $R_c = 5 a_\perp$, $\theta = \pi/2$, and $a_\perp$ ranging from 1 μm to 10 μm, N_{max} ranges from 7 to 70 atoms for a condensate of ^{87}Rb atoms ($a_{sc} = 5.77$ nm). For ^{23}Na, N_{max} is doubled (since the s-wave scattering length of ^{23}Na is $a_{sc} = 2.75$ nm).

If the attractive potential originates from a red detuned laser beam, using the estimate of Sec. VIII [Eq. (53)] one obtains $a_\perp \int_{-\infty}^{+\infty} V_\parallel(x) dx \approx 10^6$ (to be compared to the value 10^{-1} that applies to a bend). From this and from Eq. (14) it follows that for rubidium N_{max} can be as large as 10^9. In this case, however, one does not remain in the low-density regime where Eq. (14) holds [this regime is valid if $n(0) a_{sc} \ll 1$, which from Eqs. (11) and (14) gives $N_{max} \ll a_\perp/a_{sc} \sim 10^3$]. Working in the high-density regime instead, one obtains

$$N_{max} = \frac{3 a_\perp^4}{16 a_{sc}} \left| \int_{-\infty}^{+\infty} V_\parallel(x) dx \right|^3. \qquad (15)$$

One gets from this equation a value of N_{max} of the order of 10^{20}. Note, however, that in this regime the high-density approximation is valid at $x = 0$, but violated for large x (when the density tends to zero). Hence, without giving a precise order of magnitude, it is nevertheless clear from the previous estimates that the maximum number of atoms the bound state can accommodate is very large in this case.

IV. TRANSMISSION MODES

From now on we concentrate on the stationary states of a beam of condensed atoms connecting two reservoirs. For that purpose we look at the stationary solutions (in the reference frame of the laboratory) of Eq. (6) with ψ having a finite value at $x \to \pm\infty$. We write

$$\psi(x,t) = \exp\{-i\mu t\} A(x) \exp\{i\varphi(x)\} \qquad (16)$$

with A and φ real functions. Since the wave function extends to infinity, the chemical potential satisfies $\mu > \epsilon_0$. The density is $n = A^2$, and the beam velocity is $v = \varphi'$. After factorizing out the phases, Eq. (6) splits into two real equations corresponding to its imaginary and real parts. The former

imposes flux conservation, namely, the product $n(x)v(x)$ is a constant that we denote by Φ,

$$\Phi = n(x)v(x).$$

The real part gives a Schrödinger-like equation for $A(x)$,

$$-\frac{1}{2} A'' + \left[\epsilon(n) + V_\parallel + \frac{\Phi^2}{2n^2} \right] A = \mu A. \qquad (17)$$

In this section we consider the transmission modes of a condensate through a straight waveguide with no obstacle. This corresponds to solving Eq. (17) with $V_\parallel \equiv 0$. The modifications in the beam density and phase produced by the presence of an obstacle are considered in the following sections. When $V_\parallel \equiv 0$, Eq. (17) can be integrated once, yielding

$$\frac{1}{2} A'^2 + W(n) = E_{cl} \quad \text{with} \quad W(n) = -\epsilon(n) + \mu n + \frac{\Phi^2}{2n}. \qquad (18)$$

$\epsilon(n)$ in Eq. (18) is the same as in Eq. (10) and E_{cl} is an integration constant. This constant is denoted as a "classical energy" because Eq. (18) has an interpretation in terms of classical dynamics. It expresses the energy conservation of a one-dimensional Hamiltonian system for a fictitious classical particle with "position" A and "time" x moving in a potential $W(n = A^2)$, E_{cl} being the total energy of the particle. The solutions $A(x)$ therefore coincide with the "classical" solutions in the potential $W(n = A^2)$. The chemical potential μ and the flux Φ fix the shape of the potential $W(n)$, while E_{cl} selects a "trajectory" $A(x)$ in this potential.

To clarify the physical meaning of E_{cl} consider the linear (i.e., noninteracting) case $\epsilon(n) = 0$. Then the natural way to write the solution (16) is a superposition of plane waves,

$$\psi(x,t) = \exp\{-i\mu t\}[\alpha \exp(ikx) + \beta \exp(-ikx + i\theta)], \qquad (19)$$

where k is the wave vector and θ an arbitrary phase. In terms of the two real parameters α and β, the flux and the classical energy are written $\Phi = k(\alpha^2 - \beta^2)$ and $E_{cl} = k^2(\alpha^2 + \beta^2)$. E_{cl} is therefore a measure of the total intensity of the left and right incoming beams. E_{cl} can be varied while keeping Φ and μ constant [and therefore $W(n)$ constant] by changing the amplitudes α and β simultaneously while preserving the difference $(\alpha^2 - \beta^2)$.

For studying the shape of $W(n)$ in Eq. (18) in the presence of interactions it is customary to plot $\mu - dW/dn = \epsilon(n) + \Phi^2/(2n^2)$ as a function of n, as represented in the top part of Fig. 1. At low densities ($n \to 0$) the term $\Phi^2/(2n^2)$ dominates. At high densities the intra-atomic interaction contained in $\epsilon(n)$ takes over, and leads to a monotonic growth for large values of n [due to the repulsive interactions, $\epsilon(n)$ is an increasing function of n]. At intermediate values there is a minimum at a density denoted n_0. The relevant case (leading to finite densities at infinity) corresponds to $\mu \geq \epsilon(n_0) + \Phi^2/(2n_0^2)$, and is shown in Fig. 1. Then the derivative of $W(n)$ is zero for two densities n_1 and n_2, with $n_1 \leq n_0 \leq n_2$. The corresponding plot of the po-
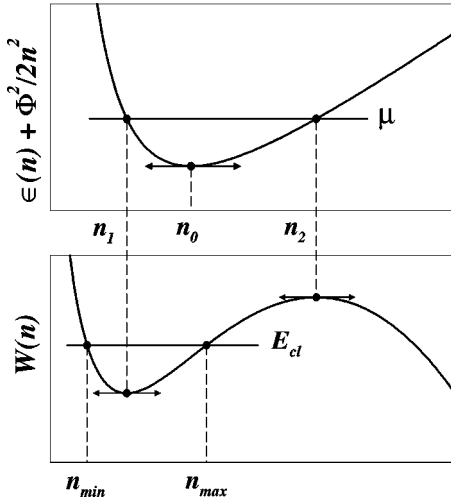
FIG. 1. Schematic behavior of the functions $\epsilon(n)+\Phi^2/2n^2$ (top part) and $W(n)$ (bottom part) as a function of n. n_i ($i=1$ or 2) is defined by $\epsilon(n_i)+\Phi^2/2n_i^2=\mu$ and is a zero of dW/dn; n_0 is a zero of the second derivative d^2W/dn^2. For given μ and Φ, a beam of uniform density has either a density n_1 [and a velocity higher than the sound velocity $c(n_1)$] or a density n_2 [and a velocity lower than $c(n_2)$]. At a given E_{cl}, n_{min} and n_{max} are the minimum and maximum values of the density oscillations [$W(n_{min})=W(n_{max})=E_{cl}$].

tential $W(n)$ is shown in the lower part of the figure. In order to have a finite density at infinity one should also impose a bounded motion of the fictitious classical particle, and this results in the two additional conditions (i) $W(n_1) \leqslant E_{cl} \leqslant W(n_2)$ and (ii) $n(x) \leqslant n_2$ for any value of x.

The different types of solution $A(x)$ are therefore described by the different motions a classical particle undergoes in a potential $W(n)$ at the allowed energies E_{cl}. The two simplest solutions correspond to the fixed points of the potential, $n(x)=n_1$ or n_2, where the "classical" particle remains at rest. They correspond to constant density solutions. Since the densities are different ($n_2 > n_1$) and the flux has the same value Φ, the velocities v_j ($j=1$ or 2) of the condensed beam are also different, with $v_2 < v_1$. v_1 (v_2) corresponds to a beam velocity above (below) the speed of sound. To see this, we first note (see below) that for a condensate *at rest* (i.e., $v \equiv 0$) with uniform density $n(x)=n$, the sound velocity c is defined by

$$c^2(n)=n\frac{d\epsilon}{dn}. \quad (20)$$

In the case of a moving condensate with uniform density n, one has a well defined velocity $v=\Phi/n$ given by $\mu=\epsilon(n)+\frac{1}{2}v^2$ [see Eq. (17)]. From Eqs. (18) and (20), moreover, we have $d^2W/dn^2=[v^2-c^2(n)]/n$. Since d^2W/dn^2 at n_1 (n_2) is positive (negative), it follows that $v_1 > c(n_1)$ [$v_2 < c(n_2)$].

We now consider the density profile of the transmission modes in the vicinity of the constant solution $n(x)=n_1$. For energies E_{cl} slightly higher than $W(n_1)$ the stationary solutions are sinusoidal waves of the form

$$A(x)=A_1+\frac{\sqrt{2}}{k}[E_{cl}-W(n_1)]^{1/2}\cos(kx+\theta), \quad (21)$$

where $k^2=d^2W/dA^2|_{A_1}=4[\Phi^2/n_1^2-c^2(n_1)]$ and $n_1=A_1^2$ is the constant density. This sinusoidal wave is reminiscent of a sound wave, but sound waves are progressive whereas Eq. (21) describes a standing wave. The structure of the sound wave (and the whole spectrum of elementary excitations) is better displayed by a slight modification of the procedure used so far. Instead of the stationary ansatz (16) one looks for solutions of the form $\psi(x,t)=\exp\{-i\mu t\}A(x-ut)\exp\{i\phi(x-ut)\}$, where u is a constant parameter, physically interpreted as the velocity of an arbitrary moving frame. Mass conservation now reads $\Phi=n(v-u)$ (Φ is the flux in the moving frame) and Eqs. (17) and (18) keep the same form, with μ replaced by $\mu+u^2/2$, all functions now depending on $X=x-ut$ and not merely on x. The constant solution $n(x)=n_1$ can now be given zero velocity ($v_1=0$) if one chooses u such that $u+\Phi/n_1=0$ (this is of importance because one wishes to study elementary excitations in a system at rest). In this case, a perturbative treatment of Eq. (18) for E_{cl} near $W(n_1)$ again gives a solution of the form (21) with x replaced by X. This is a progressive wave depending on $kX=kx-\omega_k t$ with $\omega_k=ku$, and thus satisfying the Bogoliubov dispersion relation

$$\omega_k^2=k^2\left(n_1\frac{d\epsilon}{dn}\bigg|_{n_1}+\frac{k^2}{4}\right). \quad (22)$$

The long-wavelength limit of Eq. (22) corresponds indeed to sound waves with a sound velocity $c(n_1)$ given by Eq. (20). It is also possible to obtain in this way the dispersion relation of the elementary excitations of a beam moving at constant velocity v_1 [which is simply Eq. (22) Doppler shifted].

Note that our approach is unable to reproduce the decrease of slope of the spectrum of elementary excitations that occurs in the high-density regime, for wave vectors k of the order of the transverse extension $R_\perp$ of the condensate. This effect, predicted in Refs. [24,25] and observed numerically in [26] goes beyond the quasi-1D approach: it occurs when the excitation has a wavelength allowing exploration of side regions of the condensate that have lower local sound velocity. Hence, it cannot be reproduced by using the adiabatic ansatz (1).

The structure of the stationary solutions for energies E_{cl} close to (but lower than) $W(n_2)$ is totally different from the sinusoidal waves we just discussed [which exist for $E_{cl} \gtrsim W(n_1)$]. The uniform solution $n(x)=n_2$ coexists with a solitary wave corresponding in the classical analogy to a motion along the separatrix located at $E_{cl}=W(n_2)$. This solitary wave has constant density n_2 at $x \to \pm \infty$, and a trough whose minimum density satisfies the condition $W(n_{min})=W(n_2)$ (cf. Fig. 2, top part). As the energy is lowered from $E_{cl}=W(n_2)$, density oscillations appear whose amplitude decreases as E_{cl} diminishes. These solutions are cnoidal waves (see, e.g., [27]) with periodic oscillation between two values n_{min} and n_{max}, as defined in Fig. 1. As the energy E_{cl} is
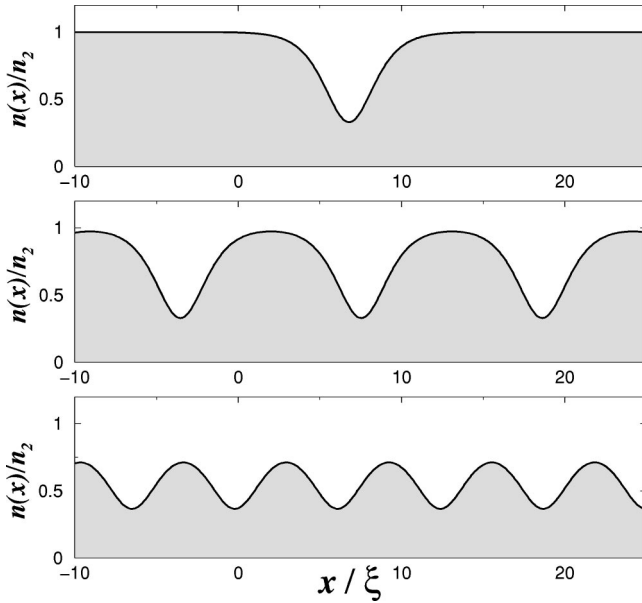
FIG. 2. Beam density along a straight guide (high-density regime) with $v_2/c_2=0.7$ [lengths are given in units of $\xi(n_2)$; see Eq. (9)]. Top: solitary wave [$E_{cl}=W(n_2)$]. Middle: cnoidal waves existing for $W(n_1)<E_{cl}<W(n_2)$. Bottom: for $E_{cl}\gtrsim W(n_1)$ the cnoidal wave deforms continuously to a sinusoidal small-amplitude wave.

further reduced the density profile tends continuously to the sinusoidal waves discussed above. This transition is illustrated in Fig. 2, which is drawn in the high-density regime for a transverse harmonic confining potential [i.e., with $\epsilon(n)$ given by Eq. (8)]. The same qualitative behavior is valid for any density regime.

Figure 2 summarizes the possible density profiles of the transmission modes of the condensate along a straight guide. In the remaining sections we consider the modifications induced by the presence of an obstacle in the flow of the condensate. Finding the transmission modes now reduces to a scattering problem in which two of the "free" modes discussed in this section are matched by the potential representing the obstacle. The correct boundary conditions to be imposed are determined by the relative value of the phase velocity

$$v_p(k)=\frac{\omega_k}{k} \qquad (23)$$

with respect to the group velocity

$$v_g(k)=\frac{\partial\omega_k}{\partial k}=v_p(k)\left(1+\frac{k^2}{k^2+4c^2(n)}\right). \qquad (24)$$

Both functions start from the value $c(n)$ at $k=0$ and then increase monotonically, with $v_g(k)>v_p(k)$ for any $k>0$. For the stationary motion of an obstacle in a condensate at rest, v_p coincides with the velocity of the obstacle with respect to the beam; this is the condition of stationarity. The energy transferred to the fluid propagates with a velocity v_g greater than the velocity of the obstacle with respect to the beam (since $v_g>v_p$). As a consequence, radiation conditions require that the wake is always located *ahead* of the obstacle (i.e., upstream in a frame where the disturbance is at rest), with no long-range perturbation of the fluid on the downstream side [28].

V. THE ATTRACTIVE SQUARE WELL

Having recalled the different solutions existing in a straight waveguide, we now discuss the influence on the transmission modes of a longitudinal potential representing a motionless obstacle placed in the trajectory of the beam. Specifically, we consider a potential $V_\parallel(x)$ that vanishes everywhere except in a finite region $0\leq x\leq\sigma$ where it takes the constant value $-V_0$ ($V_0>0$). If its origin is the presence of a bend, the square well potential corresponds to a waveguide with a constant curvature over a finite length $0<x<\sigma$ and straight elsewhere [29]. Apart from considerations related to its physical origin, this model potential is of interest because it allows one to understand in a simple case the different stationary regimes occurring also in more complex potentials.

An important point for the determination of the transmission modes of the condensate along the guide is the boundary conditions. As discussed at the end of the previous section, among all the possible stationary solutions that exist in the presence of a scattering potential, the only physical ones are those that tend to a flat density downstream. Hence we consider density profiles tending to a flat density at $x\rightarrow-\infty$, with $n(x\rightarrow-\infty)\rightarrow n_\infty$, and with a *negative* velocity $v_\infty=\Phi/n_\infty$. The sound velocity at infinity $c_\infty=c(n_\infty)$ will also be chosen negative in all the following. This corresponds to a beam incoming from the right, unperturbed far downstream by the presence of $V_\parallel$, and characterized by the two parameters v_∞ and n_∞ [or equivalently by μ and Φ, since $\mu=\epsilon(n_\infty)+v_\infty^2/2$ and $\Phi=n_\infty v_\infty$]. Moreover, we will systematically express lengths in units of $\xi=\{2[\epsilon(n_\infty)-\epsilon_0]\}^{-1/2}$ [cf. Eq. (9)].

When $V_\parallel$ is a square well, Eq. (17) takes a particularly simple form. Everything happens as for a straight waveguide, except that μ in Eq. (17) is shifted to $\mu+V_0$ in the region $0\leq x\leq\sigma$. Hence, as in the case of a straight guide, one has an integral of motion, but it takes a different value in each portion of space,

$$\frac{1}{2}A'^2+W(n)=E_{cl}^-, \qquad x\leq 0,$$

$$\frac{1}{2}A'^2+W(n)+V_0n=E_{cl}^0, \qquad 0\leq x\leq\sigma,$$

$$\frac{1}{2}A'^2+W(n)=E_{cl}^+, \qquad \sigma\leq x. \qquad (25)$$

$W(n)$ in Eq. (25) is defined as in Eq. (18). E_{cl}^-, E_{cl}^0, and E_{cl}^+ are the values of the integration constant in each region. Since the solution is flat far downstream (when $x\rightarrow-\infty$) one
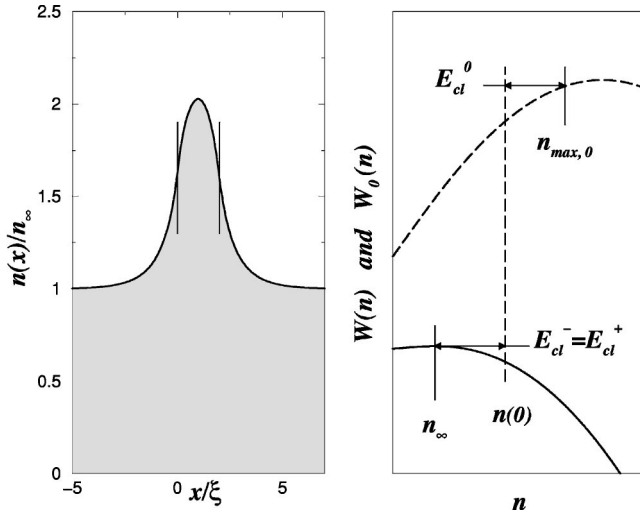
FIG. 3. Type-B stationary solution in an attractive square well. The left plot displays the density profile. The two vertical solid lines indicate the location of the square well. This plot corresponds to $\sigma=2\xi$ and $V_0\xi^2=0.5$ in a low-density beam at velocity $v_\infty/c_\infty=0.7$ [the healing length ξ is defined as in Eq. (9) and is computed at density n_∞]. The right plot illustrates the behavior of the solution in the diagram $(n,W(n))$. The solid curve represents $W(n)$ and the dashed one $W_0(n)$. In the rear of the obstacle, the density evolves from n_∞ to $n(0)$ in the potential $W(n)$ with a classical energy $E_{cl}^-=W(n_\infty)$, then from $n(0)$ to $n_{max,0}$ and back to $n(0)$ in the potential $W_0(n)$ (with energy E_{cl}^0), and finally the upstream density goes from $n(0)$ to n_∞ in $W(n)$.

has $E_{cl}^-=W(n_\infty)$. The matching at $x=0$ and $x=\sigma$ imposes continuity of the density and of its derivative. This leads to

$$E_{cl}^- + V_0 n(0) = E_{cl}^0 = E_{cl}^+ + V_0 n(\sigma). \qquad (26)$$

Different types of solution satisfying Eqs. (25) exist, depending whether the far downstream beam velocity v_∞ is greater or smaller than the speed of sound $c(n_\infty)=c_\infty$. We consider these two different regimes separately.

A. Low beam velocity: $v_\infty/c_\infty<1$

The first type of solution we consider is rather intuitive if employing a perturbative treatment (see Sec. VII). It corresponds to solutions with an increased density in the region of the potential. In the following, we refer to these solutions as B solutions (where B stands for bump).

The B solutions are found by looking for solutions with a density increasing when x moves from $x=-\infty$ toward the origin. Since at $x\to-\infty$ the density has the constant value n_∞, and since we are imposing $v_\infty/c_\infty<1$, n_∞ coincides with the uniform density denoted n_2 in Sec. IV, and $E_{cl}^-=W(n_\infty)$. But unlike the solitary wave of Sec. IV in which the density decreases, in a type-B solution we move to the right of $n_\infty=n_2$ along the separatrix (see Fig. 3) and the B solution has a density peak instead of a trough.

Since the boundary conditions are fixed downstream, here and in all the following we find it more convenient to integrate Eqs. (25) starting far in the rear of the obstacle, i.e., from left infinity (remember that the beam is incident from

the right). Starting from a value n_∞ at $x=-\infty$, the density has reached a value $n(0)$ at $x=0$. From this point on the equivalent "classical particle" moves in the potential

$$W_0(n)=W(n)+V_0 n \qquad (27)$$

at an energy $E_{cl}^0=E_{cl}^- + V_0 n(0)$. At $x=\sigma$ it evolves again in $W(n)$. Since to reach a finite density when $x\to+\infty$ one needs to have $E_{cl}^+\leq W(n_\infty)=E_{cl}^-$, from Eq. (26) this imposes $n(\sigma)\geq n(0)$. But, if the inequality is strict, one has $E_{cl}^+ < W(n_\infty)$ and $n(\sigma)>n(0)\geq n_\infty$: this case should be excluded since from Fig. 1 one sees that this leads to a diverging density at right infinity (the classical particle escapes to infinity). Hence one should have $n(0)=n(\sigma)$, $E_{cl}^+=E_{cl}^-$ and the B solutions are even.

These solutions exist for any type of attractive square well. For a given beam (characterized by n_∞ and v_∞) and given values of σ and V_0, the value of $A(0)$ is determined by demanding that the amplitude varies from $A(0)$ to its maximum value $A_{max,0}$ and back over a distance σ. $A_{max,0}$ is determined as a function of $A(0)$ from the equation $W_0(A)=E_{cl}^0$ whose two smallest positive solutions are denoted $A_{min,0}$ and $A_{max,0}$ (in all the following we denote with an index "0" the quantities concerning W_0 and defined as for W in Fig. 1). We have

$$\sigma=2\int_{A(0)}^{A_{max,0}}\frac{dA}{A'}=\sqrt{2}\int_{A(0)}^{A_{max,0}}\frac{dA}{\sqrt{E_{cl}^0-W_0(A)}}. \qquad (28)$$

For sufficiently small σ the only existing B solution is the one described above. However, new B solutions appear as the width σ increases, because the "classical particle" before evolving back in $W(n)$ has enough "time" to make one (or several) oscillations in $W_0(n)$. The general density profile of the B type increases from n_∞ at $x=-\infty$, up to $x=0$, and has N maxima and $N-1$ minima between $x=0$ and $x=\sigma$, with $N=1,2,3\ldots$ We denote this a B_N solution. Figure 3 corresponds to a B_1 solution. The behavior of a B_2 solution is illustrated in Fig. 4. For an arbitrary N, Eq. (28) takes the form

$$\sigma=2\int_{A(0)}^{A_{max,0}}\frac{dA}{A'}+2(N-1)\int_{A_{min,0}}^{A_{max,0}}\frac{dA}{A'}, \qquad (29)$$

where $A_{min,0}$ and $A_{max,0}$ are, as indicated before, the two smallest positive solutions of $W_0(A)=E_{cl}^0$. The width of the potential below which a given solution disappears occurs when $A(0)=\sqrt{n_\infty}=A_{max,0}$. In this case the solution is perfectly flat for $x\leq 0$ and $x\geq \sigma$ and is a portion of a cnoidal wave (with N oscillations) in the region $0\leq x\leq \sigma$. For a given V_0, this forces σ to be larger than the value $\sigma_N(V_0)$,

$$\sigma\geq\sigma_N(V_0)=\sqrt{2}(N-1)\int_{\sqrt{n_\infty}}^{A_{max,0}}\frac{dA}{\sqrt{E_{cl}^0-W_0(A)}}. \qquad (30)$$

Other types of solution, different from the B family, exist for a beam velocity lower than the speed of sound. They correspond to density profiles that *decrease* from the down-
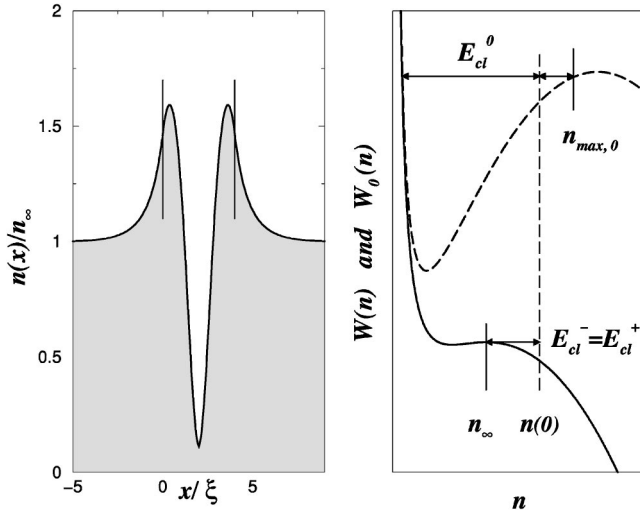
FIG. 4. A B_2 solution in an attractive square well. Left and right parts as in Fig. 3. The plot corresponds to $\sigma = 4\xi$ and $V_0 \xi^2 = 0.5$ in a low-density beam at velocity $v_\infty/c_\infty = 0.7$. The downstream density evolves from n_∞ to $n(0)$ in the potential $W(n)$ with a classical energy $E_{cl}^- = W(n_\infty)$; then it makes a complete oscillation in $W_0(n)$ starting from $n(0)$ toward $n_{max,0}$ and ending again at $n(\sigma) = n(0)$. Finally, the upstream density goes from $n(\sigma)$ to n_∞ in the potential $W(n)$.

FIG. 5. A D_1 solution in an attractive square well. Left and right parts as in Fig. 3. Plot (a) is the generic case [with $n(\sigma) > n(0)$] and (b) is the symmetric case where $n(\sigma) = n(0)$. These plots correspond to $\sigma = 2\xi$ and $V_0 \xi^2 = 0.1$ in a low-density beam at velocity $v_\infty/c_\infty = 0.7$. The right plot illustrates the behavior of the typical solution [such as displayed in part (a)] in the diagram $(n, W(n))$. The downstream density evolves from n_∞ to $n(0)$ in the potential $W(n)$ with a classical energy $E_{cl}^- = W(n_\infty)$; then in W_0 (with an energy E_{cl}^0) from $n(0)$ to the minimum density $n_{min,0}$ and back to a value $n(\sigma)$ [larger than $n(0)$]. Finally, the upstream density oscillates in the classical potential $W(n)$ as a cnoidal wave.

stream asymptotic value n_∞ as x moves from $-\infty$ toward the origin, with $E_{cl}^- = W(n_\infty)$. Hence this type of solution is a portion of a solitary wave in the rear of the obstacle. We refer to these solutions as the D solutions (where D stands for depressed).

For a D solution, the density has a value $n(0) < n_\infty$ at $x = 0$ and from there on the equivalent classical particle evolves in the potential W_0. In the simplest case the particle bounces once on the repulsive core at the origin, namely, the density further decreases until it reaches a value $n_{min,0}$ [satisfying $E_{cl}^0 = W_0(n_{min,0})$] and then increases until $x = \sigma$. Then the classical particle evolves in $W(n)$ again, with an energy E_{cl}^+ that has to be lower than or equal to $W(n_\infty)$, and this imposes $n(\sigma) \geq n(0)$ [cf. Eq. (26)]. Note that here, contrary to the case of the B solution, the strict inequality is possible; it corresponds to $E_{cl}^+ < W(n_\infty)$ and $n(\sigma) < n_\infty$, i.e., the upstream solution is a cnoidal wave. In the particular case that $n(\sigma) = n(0)$ the solution is even. A generic density profile with a cnoidal wave is represented in Fig. 5(a), and the even solution is represented in Fig. 5(b).

For a given well depth V_0 the simple D solutions of Fig. 5 (which we denote as the D_1 solutions, with one minimum in the region of the potential) do not exist for all values of σ. When the well becomes very large, σ may exceed the period of the oscillation of density in the well (i.e., the "time" period of the "classical particle" evolving in W_0). In that case the D_1 solution disappears. The limiting case corresponds to $n(0) = n_\infty = n(\sigma)$, i.e., to a flat density outside the region of the well having one oscillation in the region of the well. This upper limit is exactly the lower limit $\sigma_2(V_0)$ below which the B_2 solution does not exist. As a consequence, when σ increases from a small value the D_1 solution disappears at
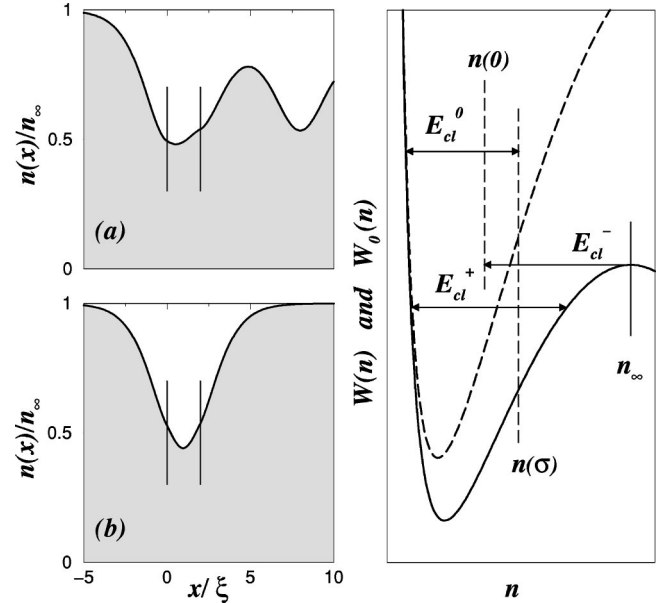
$\sigma = \sigma_2(V_0)$ and becomes the B_2 solution (of the type illustrated in Fig. 4), which is then allowed for any larger value of σ. The point is that for a B solution, when changing from potential W to W_0 in the (n, W) diagram, one can jump arbitrarily close to the separatrix of W_0, thus making the period in the region of the potential as large as desired. Hence, once a B solution exists for a given σ, it exists also for any larger value. For a D solution, however, the period in W_0 is limited: it takes its largest value if one enters and leaves the region of the potential W_0 with a flat density [i.e., $n(0) = n_\infty = n(\sigma)$].

The existence of the D_1 solution for $\sigma < \sigma_2(V_0)$ depends on the value of V_0 and of the relative positions of the curves $W(n)$ and $W_0(n)$ in the (n, W) diagram. One regime is set by small values of V_0 such that the condition $n_{min} < n_{1,0}$ is satisfied, where n_{min} is the smallest positive solution of $W(n) = W(n_\infty)$ [see Fig. 1 in the case $E_{cl} = W(n_2 = n_\infty)$] and $n_{1,0}$ is the first zero of dW_0/dn (remember that we denote with an index "0" the quantities concerning W_0 and defined as in Fig. 1 for W). In this case one can easily check that any value of σ smaller than $\sigma < \sigma_2(V_0)$ corresponds to an acceptable B_1 solution. On the contrary, for larger values of V_0 for which $n_{min} > n_{1,0}$ is satisfied there is a minimum width $\sigma_1^*(V_0)$ below which D_1 solutions do not exist:

$$\sigma_1^*(V_0) = \sqrt{2} \int_{A_{min,0}}^{A_{max,0}} \frac{dx}{\sqrt{E_{cl}^0 - W_0(n)}}, \quad (31)$$
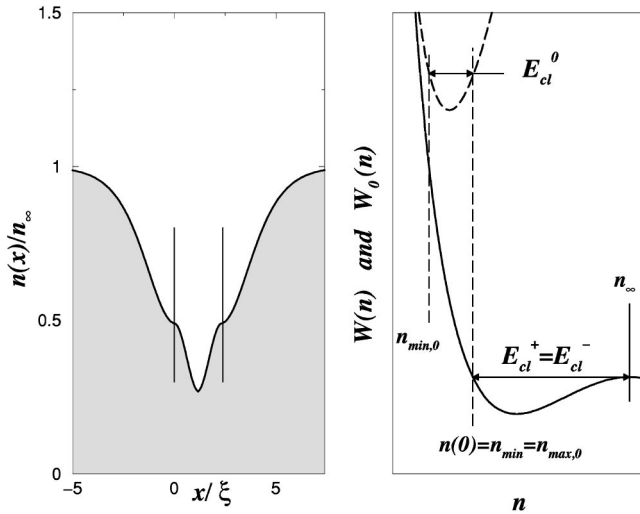
FIG. 6. The D_1 solution in a strongly attractive square well of width just above $\sigma_1^*(V_0)$. Left and right parts as in Fig. 3. The density outside the well is composed of two half solitons. This plot corresponds to $V_0\xi^2 = 0.5$ and $\sigma \approx 2.4\xi$ in a low-density beam at velocity $v_\infty/c_\infty = 0.7$. The density evolves from n_∞ (far downstream) to $n(0) = n_{min}$ in the potential $W(n)$ with classical energy $E_{cl}^- = W(n_\infty)$. It then evolves in W_0 from $n(0)$ to $n_{min,0}$ and back. Finally, the upstream density oscillates in the classical potential $W(n)$ from $n(\sigma) = n_{min}$ back to n_∞.

where $E_{cl}^0 = W(n_{min}) + V_0 n_{min}$, $A_{min,0}$ and $A_{max,0}$ being solutions of $W_0(A) = E_{cl}^0$ (one has $A_{max,0} = A_{min}$). The limiting case $\sigma = \sigma_1^*(V_0)$ is illustrated in Fig. 6. The situation for the solutions of type D_1 is summarized in Fig. 7.

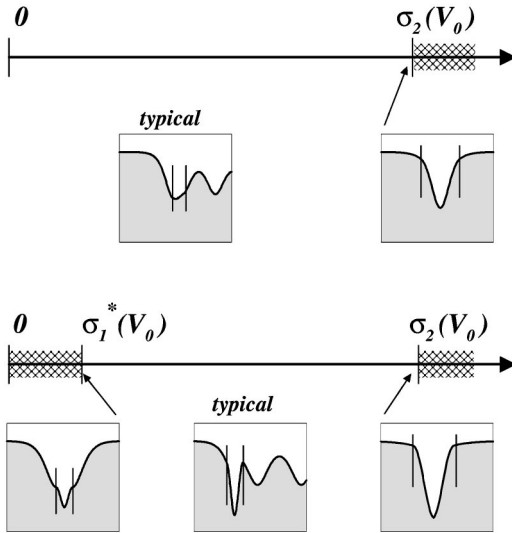
FIG. 7. Synoptic diagram of the evolution of the morphology of the D_1 solution for a given V_0, as σ increases. The insets display the density profiles $n(x)/n_\infty$. Hatched regions indicate values of σ for which the solution does not exist. For shallow potentials (for which $n_{1,0} > n_{min}$, upper part of the plot) the D_1 solution exists for any width σ between 0 and $\sigma_2(V_0)$. For deep potential ($n_{1,0} < n_{min}$, lower part) it exists only if $\sigma \in [\sigma_1^*(V_0), \sigma_2(V_0)]$. In both cases (shallow or deep potentials) at $\sigma = \sigma_2(V_0)$ the D_1 solution disappears and becomes a B_2 solution.

D solutions can oscillate in the region of the well, as B solutions do. We denote by D_N solution a type-D solution with N minima. Contrary to the case of B_N solutions, there exists a maximum width for D_N solutions to occur. When the D_N solution disappears, it becomes a B_{N+1} solution (exactly as discussed above for $N=1$). D_N solutions are not necessarily even as B_N solutions are; ahead of the obstacle (for $x \gtrsim \sigma$) they typically consist of a cnoidal wave (see the discussion for $N=1$ and Fig. 5). In this case we do not consider that the minima of the cnoidal wave outside the well increase the index N in the name D_N solution [for instance, the profile of Fig. 5(a) corresponds to a D_1 solution although an infinity of minima occur upstream]. Furthermore, D_N solutions have the additional feature that they may not exist for values of σ lower than $\sigma_N(V_0)$. This was explained above in detail for the case $N=1$. Figure 8 illustrates this generic behavior for a D_2 solution.

As for $N=1$, for this family there are generically two main types of potential well, depending whether $n_{1,0}$ is larger (shallow potential) or smaller (deep potential) than n_{min} (left and right parts of Fig. 8, respectively). In the case of a shallow potential the D_2 solution exists for any width below $\sigma_3(V_0)$; this is not the case for deep potentials. We will not comment on Fig. 8 in great detail, but we note that even in the simple case of a shallow potential interesting bifurcations occur. Let us focus on this case. For simplicity we discard from the discussion solutions forming cnoidal waves upstream (i.e., for $x \gtrsim \sigma$). Then, for small widths, the only possible D_2 solutions are even. For a certain width the minima of density occur exactly at $x=0$ and $x=\sigma$ [it is easy to see that this width coincides with $\sigma_1^*(V_0)$ defined in Eq. (31)]. From there on, the previous even solutions still exist, but new solutions appear. They correspond to a portion of a soliton with its minimum before the well and one portion of cnoidal oscillation inside the well (see Fig. 8, left part). This solution is degenerate in the sense that there exists a symmetrical equivalent solution (where the minimum of the soliton occurs beyond the well). It disappears when $\sigma = \sigma_2(V_0)$. For σ just below this value, one has exactly one soliton out of the well and one cnoidal oscillation inside the well; hence the trough of the solitonic part of the solution is sent to infinity (a feature that is not clearly seen on Fig. 8 due to numerical difficulties). For larger values of σ one has to oscillate more than once in the region of the well, but these are D_3 and not D_2 solutions. On the other hand, the even solutions still exist until $\sigma = \sigma_3(V_0)$. The situation is slightly more complicated for deep potentials, but the basic ingredients are the same as for shallow potentials and we present the different allowed density profiles in Fig. 8 (right part) without detailed discussion.

B. High beam velocity: $v_\infty/c_\infty > 1$

We now consider beam velocities v_∞ larger (in absolute value) than $c_\infty = c(n_\infty)$. In the language of Fig. 1, n_∞ is in this case of type n_1 (the minimum of the potential) and $E_{cl}^- = W(n_1)$. The only possible flat solution far in the rear of the obstacle is a flat and constant density, namely, $n(x \lesssim 0) = n_\infty$. The matching condition (26) yields $E_{cl}^+ = E_{cl}^-$
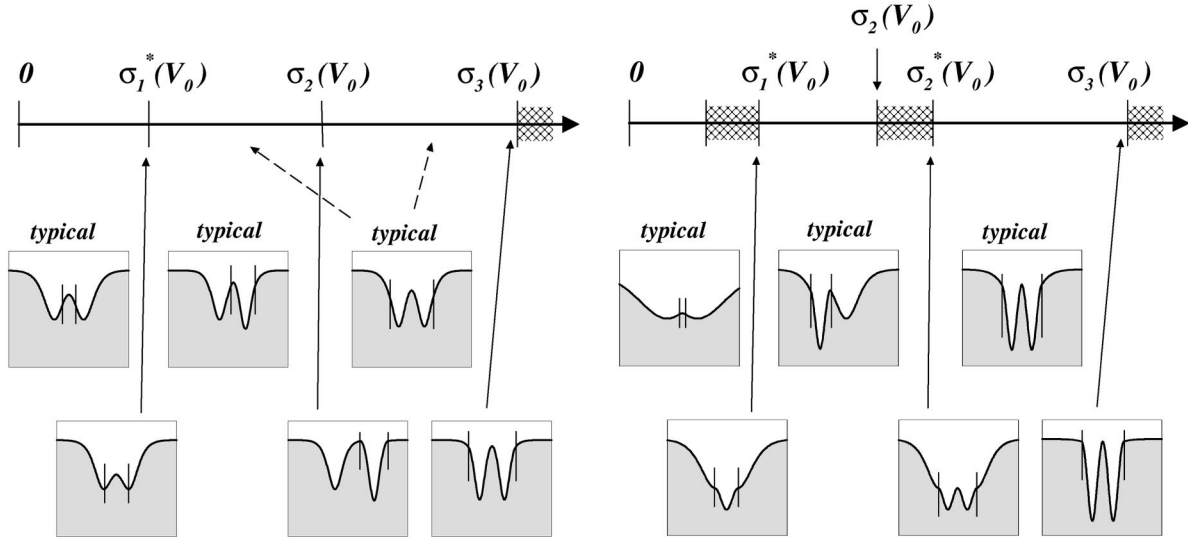
FIG. 8. Synoptic diagram of the evolution of the morphology of the D_2 solution for given V_0, as σ increases (see caption of Fig. 7). For σ larger than $\sigma_3(V_0)$ the D_2 solution disappears (it becomes a B_3 solution). The left part corresponds to a shallow well and the right part to a deep well. For legibility, the cases denoted as ''typical'' have been taken to consist ahead of the obstacle (for $x \geq \sigma$) of a portion of a soliton (whereas the most generic solutions are cnoidal waves).

$+V_0[n_\infty - n(\sigma)]$. One should verify that $E_{cl}^+ \geq W(n_1 = n_\infty) = E_{cl}^-$ (see Fig. 1) and this imposes $n(\sigma) \leq n_\infty$. This inequality is trivially satisfied, because the solution inside the well is a cnoidal wave with $n_{max,0} = n_\infty$ (see Fig. 9). If we denote by n_2 (as in Sec. IV) the second zero of dW/dn (the first one being $n_1 = n_\infty$) one has also to verify that $E_{cl}^+ \leq W(n_2)$. This imposes

$$n(\sigma) \geq n_{\sigma,inf} = n_\infty - \frac{1}{V_0}[W(n_2) - W(n_1)]. \qquad (32)$$

Once this condition is fulfilled, the upstream solution is a cnoidal wave. Because these solutions have a constant downstream density, we denote them C solutions.

Two different cases are to be considered. The first and simpler one corresponds to $n_{min,0} > n_{\sigma,inf}$. It occurs for high beam velocity [when $W(n_2) - W(n_1)$ is large] and for shallow potentials (when V_0 is small). In that case, the density of the cnoidal wave inside the well oscillates between $n_{min,0}$ and $n_{max,0}$, and the matching at $x = \sigma$ is always possible. The incoming wave (for $x \geq \sigma$) is a cnoidal wave corresponding to oscillations of the ''classical particle'' in the potential $W(n)$. This behavior is illustrated in Fig. 9(a).

The other case corresponds to $n_{\sigma,inf} > n_{min,0}$. Then all the widths are not acceptable, namely, σ should be such that $n(\sigma) > n_{\sigma,inf}$. If one denotes by L_a the length the density takes to go from the value $n_{\sigma,inf}$ to $n_{max,0}$ and by L_0 the period of the cnoidal wave in the well, one has

$$L_a = \frac{1}{\sqrt{2}} \int_{\sqrt{n_{\sigma,inf}}}^{\sqrt{n_{max,0}}} \frac{dA}{\sqrt{E_{cl}^0 - W_0(A)}} \quad \text{and}$$

$$L_0 = \sqrt{2} \int_{\sqrt{n_{min,0}}}^{\sqrt{n_{max,0}}} \frac{dA}{\sqrt{E_{cl}^0 - W_0(A)}}. \qquad (33)$$

The allowed values of σ are in the intervals $[0, L_a] \cup [L_0 - L_a, L_0 + L_a] \cup [2L_0 - L_a, 2L_0 + L_a] \cup \cdots$.

The region of validity of the first case $n_{min,0} > n_{\sigma,inf}$ can be evaluated analytically in the low-density regime. In this regime one obtains $W(n_2) - W(n_1 = n_\infty) = n_\infty F(v_\infty/c_\infty)/(4\xi^2)$ where

$$F(z) = \left[\frac{z^2}{4} \left(1 + \sqrt{1 + \frac{8}{z^2}} \right) - 1 \right] \left[\frac{5z^2}{4} + 1 - \frac{3z^2}{4} \sqrt{1 + \frac{8}{z^2}} \right]. \qquad (34)$$

This yields $n_{\sigma,inf}/n_\infty = 1 - F(z)/(4V_0\xi^2)$ (we set $z = v_\infty/c_\infty$). One also obtains $n_{min,0}/n_\infty = G(z, V_0\xi^2)$ where

$$G(z, V_0\xi^2) = \frac{z^2 + 1}{2} + 2V_0\xi^2 - \sqrt{\left(\frac{z^2 + 1}{2} + 2V_0\xi^2 \right)^2 - z^2}. \qquad (35)$$

The region of validity of the condition $n_{\sigma,inf} < n_{min,0}$ (where all the potential widths are acceptable) can be displayed in a diagram $(z = v_\infty/c_\infty, V_0\xi^2)$. It corresponds to the region

$$1 - \frac{F(z)}{4V_0\xi^2} < G(z, V_0\xi^2), \qquad (36)$$

i.e., to the domain below the solid line in Fig. 10.

VI. THE REPULSIVE SQUARE WELL

In this section we consider a simple repulsive potential, namely, we take $V_\parallel(x)$ to be zero everywhere except in a finite region $0 \leq x \leq \sigma$ where it takes the constant value V_0 ($V_0 > 0$). This type of potential cannot correspond to a bend in the guide, but it can be realized with a (blue detuned) far-off-resonant laser field.
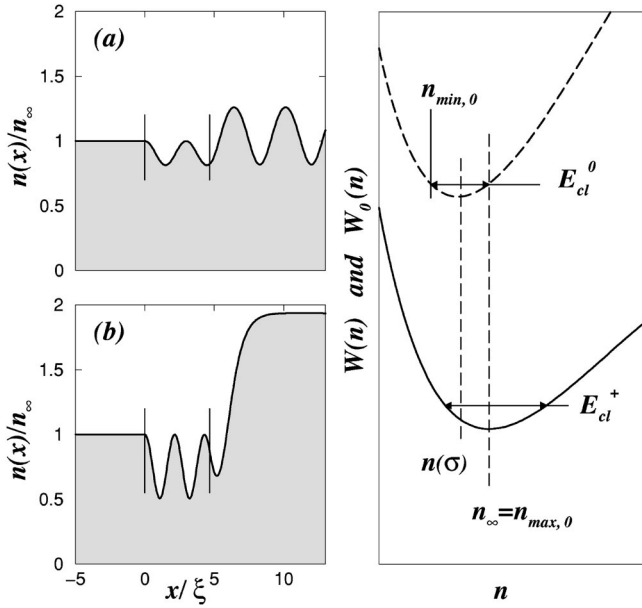
FIG. 9. A C solution in an attractive square well. Left and right parts as in Fig. 3. Both density plots in the left part concern a low-density beam, with $v_\infty/c_\infty=1.6$ and a square well of width $\sigma/\xi=4.68174$. Plot (a) is the generic case and corresponds to $V_0\xi^2=0.1$. For these values of V_0 and v_∞ the condition (32) is fulfilled for any σ. Plot (b) corresponds to a well of depth $V_0\xi^2=0.5$. The parameters have been chosen in this case such that $E_{cl}^+=W(n_2)$ and the C solution is just about to disappear. The right plot illustrates the behavior of the typical solution [corresponding to part (a)] in the diagram $(n,W(n))$. The density is constant and equal to n_∞ for $x\leq0$ in $W(n)$. From $x=0$ to $x=\sigma$ the "classical particle" evolves in $W_0(n)$ (with an energy E_{cl}^0). Finally, the upstream density oscillates in the classical potential $W(n)$ as a cnoidal wave.

Equation (25) still holds after changing the sign of V_0. Equation (26) holds also, but we rewrite it here with the appropriate sign for future reference,

$$E_{cl}^- - V_0 n(0)=E_{cl}^0=E_{cl}^+-V_0 n(\sigma), \qquad (37)$$

and similarly one has here [instead of Eq. (27)]

$$W_0(n)=W(n)-V_0 n. \qquad (38)$$

The potential $W_0(n)$ has, for V_0 relatively small, the same behavior as $W(n)$, namely, one minimum at $n_{1,0}$ and one maximum at $n_{2,0}$, with $n_1<n_{1,0}<n_0<n_{2,0}<n_2$ (the notations are defined in Sec. IV, see Fig. 1). On the other hand, for large V_0, W_0 is a monotonically decreasing function of n. The transition between the two regimes occurs when $\mu-V_0=\epsilon(n_0)+\Phi^2/(2n_0^2)$. Hence, the terms "low" or "large" V_0 we just defined (we also speak below of "weak" and "strong" potentials) are not intrinsic properties of the potential, but depend on the chemical potential μ and on the flux Φ of the incoming beam (this remark is made quantitative in Sec. VI A below).

Among all the possible solutions, we choose again to select those corresponding to a flat density at left infinity [$n(x)\rightarrow n_\infty$ as $x\rightarrow-\infty$] with a negative velocity [$v(x)$
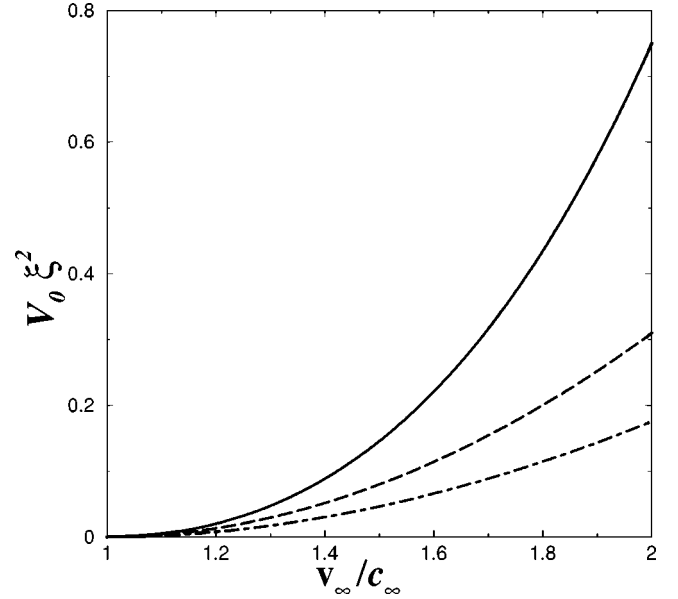

FIG. 10. Representation (for low-density beams) of the part of the plane (v_∞,V_0) where the C solution is allowed for any potential width. The allowed region is located below the solid curve. We also display on the same diagram the region where C solutions are allowed for any width of a *repulsive* potential (see Sec. VI A). It corresponds to the domain below the dashed curve for low-density beams and below the dot-dashed one for high-density beams.

$\rightarrow v_\infty<0$]. Under these conditions, the transmission modes through repulsive potentials appear to be simpler than the attractive ones discussed in Sec. V, as we are now going to show.

A. High beam velocity: $v_\infty/c_\infty>1$

The stationary solutions of a supersonic beam encountering a repulsive square well have important similarities with the C solutions of Sec. V and will be given the same name. For weak potentials [$V_0<\mu-\epsilon(n_0)+\Phi^2/(2n_0^2)$] the solutions exist whatever the value of σ, and their shape is very similar to the transmission mode illustrated in Fig. 9(a). The main difference is that here one has $n(x)\geq n(0)=n_\infty$ in the region of the well (whereas the reverse inequality holds for C solutions in an attractive well).

On the other hand, for strong potentials the solution in the region of the well is not (as for weak potentials) a cnoidal wave. In this region the density increases monotonically from $x=0$ up to $x=\sigma$; then "classical" motion occurs in $W(n)$ and the upstream density profile further oscillates as a cnoidal wave. This means that there exists a maximum value of σ above which no solution can be found in a strong potential. When σ reaches this maximum value, the solution for $x\geq\sigma$ is a portion of a soliton and the whole solution has a steplike shape going from $n_\infty=n_1$ (far in the rear of the obstacle) up to n_2 at $x\rightarrow+\infty$. The behavior in this limiting case is illustrated in Fig. 11. There is here a difference with the case of a strong attractive square well: when σ has exceeded this maximum value, no other stationary solution appears for larger widths. The reason is that in an attractive
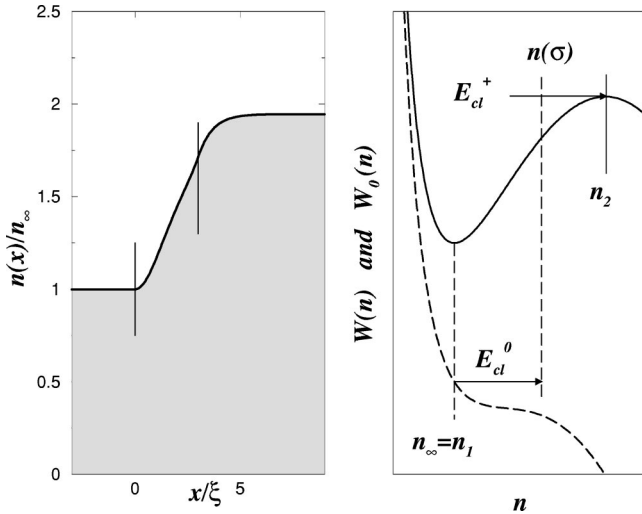
FIG. 11. A C solution in a repulsive square well. The parameters have been chosen in this case such that $E_{cl}^+ = W(n_2)$ and the C solution is just about to disappear. Left and right parts as in Fig. 3. The left plot concerns a low-density beam, with $v_\infty / c_\infty \simeq 1.6$, and a square well of width $\sigma/\xi = 3$ and depth $V_0 \xi^2 = 0.1$. The right plot illustrates the behavior of this solution in the diagram $(n, W(n))$. The downstream density is constant and equal to n_∞. From $x=0$ to $x=\sigma$ the "classical particle" evolves in $W_0(n)$ (with an energy E_{cl}^0); then it evolves back in $W(n)$, just on the separatrix.

square well, the solution in the region of the well is periodic, whereas it increases here without limit for large wells.

Due to the similarities with the case of an attractive potential, it is interesting here also to determine more precisely for which beams a stationary supersonic solution can be found (for weak potentials) for all values of σ. An analytical treatment is here possible in both the low- and high-density regimes. The two cases can be treated on the same footing by introducing an index ν with $\nu=1$ in the dilute regime and $\nu=1/2$ for high densities. One has

$$\epsilon(n) = \epsilon_0 + \frac{1}{2\xi^2}\left(\frac{n}{n_\infty}\right)^\nu \quad \text{and} \quad v^2 = \frac{\nu z^2}{2\xi^2}\left(\frac{n_\infty}{n}\right)^2, \quad (39)$$

where $z = v_\infty / c_\infty$. One then obtains $n_0/n_\infty = z^{2/(\nu+2)}$ (n_0 is defined in Sec. IV, Fig. 1). The condition for a repulsive potential to be considered as weak is thus $\mu - V_0 \geq \epsilon(n_0) + \Phi^2/(2n_0^2) = \epsilon_0 + (n_0/n_\infty)^\nu(1+\nu/2)/(2\xi^2)$. Since $\mu = v_\infty^2/2 + \epsilon(n_\infty)$, this reads

$$V_0 \xi^2 \leq \frac{1}{2} + \frac{\nu z^2}{4} - \frac{1}{2}\left(1 + \frac{\nu}{2}\right)z^{2\nu/(\nu+2)}. \quad (40)$$

This region of weak potential corresponds in Fig. 10 to the domain below the dashed curve in the dilute regime $\nu=1$, and below the dot-dashed curve in the high-density regime $\nu=1/2$. As stated in the beginning of this section, the terms weak or strong potential do not characterize an intrinsic property of the well. At $v_\infty = c_\infty$, for instance, all the potentials are "strong."

In view of future experimental studies of the system, it is also interesting to determine (in the regime of "strong poten-

tials") the critical value of σ after which no C solution can be found. We denote this value by L_r. Following a reasoning similar to the one of Sec. V B one obtains

$$L_r = \frac{1}{\sqrt{2}} \int_{\sqrt{n_{min,0}}}^{\sqrt{n_{\sigma,sup}}} \frac{dA}{\sqrt{E_{cl}^0 - W_0(A)}}$$

$$\text{where} \quad n_{\sigma,sup} = n_\infty + \frac{1}{V_0}[W(n_2) - W(n_1)]. \quad (41)$$

In the low-density regime L_r can be expressed in terms of an elliptic integral:

$$\frac{L_r}{\xi} = \int_0^{F(z)/(4V_0\xi^2)} \frac{dx}{\sqrt{2x}[x^2 + x(4V_0\xi^2 + 1 - z^2) + 4V_0\xi^2]^{1/2}}$$

$$\simeq \frac{1}{V_0\xi^2}\left(\frac{F(z)}{8}\right)^{1/2}. \quad (42)$$

Note, of course, that Eq. (42) is meaningful only when the condition (40) is violated. L_a in Eq. (33) can also be defined with a similar expression in the low-density regime. Both expressions are well approximated by the left part of Eq. (42), meaning that one has $8(L_{r/a}V_0\xi)^2 \simeq F(z)$. We will see below that this corresponds to approximating the potential by a δ function [cf. Sec. VII, Eq. (50)].

B. Low beam velocity: $v_\infty/c_\infty < 1$

It is easy to check that in this case only D_1 solutions can be observed (there are no other D solutions, and B solutions are forbidden). The downstream solution starts at left infinity from a density n_∞ which is of type n_2 in the terminology of Sec. IV. $n(x)$ decreases from this value, and in the diagram $(n, W(n))$ the fictitious classical particle evolves in the potential $W_0(n)$ during a "time" σ, and then evolves in $W(n)$ again. Since one should verify that $E_{cl}^+ \leq W(n_2) = E_{cl}^-$, from Eq. (37) this imposes $n(\sigma) \leq n(0)$. If the inequality is strict, the solution for $x > \sigma$ is a cnoidal wave. If $n(\sigma) = n(0)$ the final solution is a portion of a soliton.

Let us consider a strong potential first. If the well is narrow ($\sigma \to 0$), there are two possible solutions, depending on whether, in the diagram $(n, W(n))$, one "jumps" rapidly or not from W to W_0. This is illustrated on Fig. 12. When σ increases, these two solutions merge and disappear. This behavior was already observed by Hakim in the case of a model repulsive δ potential [30]. Hakim showed (for the one dimensional Gross-Pitaevskii equation, i.e., in the dilute regime) that the solution that "jumps late" to W_0 (right part of Fig. 12) is unstable, and argued convincingly that the other is stable. The same situation is expected to occur here.

In the case of a weak potential there are also two types of solution, but they do not disappear when σ increases. The point is that one can have here E_{cl}^0 arbitrarily close to the separatrix energy $W_0(n_{2,0})$, and the period of motion in the potential W_0 can thus be made as large as desired. From Eq. (37), one has $E_{cl}^0 = W_0(n_{2,0})$ if $n(0) = n_0^*$ with
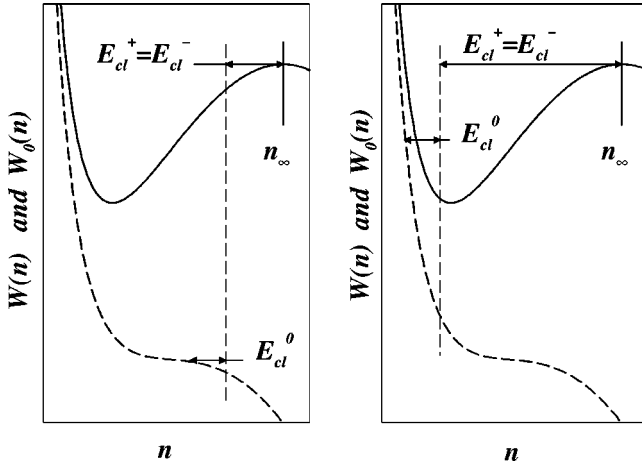
FIG. 12. Schematic representation in the $(n,W(n))$ diagram of the behavior of D_1 solutions in a strong repulsive square well $(v_\infty/c_\infty<1)$. The solid curve represents $W(n)$ and the dashed one $W_0(n)$. For this type of potential there are two possible solutions for a given value of the width σ (as discussed in the text). This is illustrated by the figure, namely, the ''time'' the fictitious particle spends in the potential W_0 is the same in the left and right plots. For simplicity, the examples we give here are drawn in the particular case $n(0)=n(\sigma)$.

$$n_0^* = n_{2,0} + \frac{1}{V_0}[W(n_2)-W(n_{2,0})]. \tag{43}$$

The expression ''jumping soon'' (or ''late'') from W to W_0 that we used in the discussion of strong potentials refers, for a weak potential, to the case where $n(0)>n_0^*$ [or $n(0)<n_0^*$]. If $n(0)>n_0^*$, the density remains larger than $n_{2,0}$ and

reaches this value at its minimum in the limit $\sigma\to\infty$. If $n(0)<n_0^*$, $E_{cl}^0>W_0(n_{2,0})$, and the fictitious classical particle evolves above the separatrix in the potential W_0. As in the case of a strong potential, this solution is expected to be unstable. The other one is certainly stable since one can show that it is identical to the result of perturbation theory in the limit of a very weak potential.

VII. SIMPLE SOLUTIONS IN THE PRESENCE OF AN OBSTACLE

The aim of this section is to study, by means of perturbation theory, some simple solutions of Eq. (17) valid for a generic potential $V_\parallel(x)$. We will argue that near the speed of sound this approach fails, and that in this regime any potential can be approximated by a δ peak. We will then study the scattering modes of the condensate in the presence of this potential. It allows for a qualitative and simple understanding of the solutions obtained for more realistic potentials in the previous sections. Some of the results presented here have already been obtained by Hakim [30], who considered repulsive potentials only, in a slightly less general setting.

We again restrict the analysis to those transmission modes tending to a flat density at $x\to-\infty$, $n(x\to-\infty)\to n_\infty$, with a negative velocity v_∞. These are of the form $A(x)=A_\infty+\delta A(x)$ (with $A_\infty^2=n_\infty$). Denoting by c_∞ the sound velocity at density n_∞ [Eq. (20)], a perturbative treatment of Eq. (17) yields

$$\delta A'' + 4(v_\infty^2-c_\infty^2)\delta A = 2A_\infty V_\parallel(x). \tag{44}$$

The solutions of Eq. (44) that tend to zero when $x\to-\infty$ are of the form

$$\delta A(x)=\begin{cases} -\dfrac{A_\infty}{k}\displaystyle\int_{-\infty}^{+\infty} V_\parallel(y)\exp\{-k|x-y|\}dy & \text{when} \quad v_\infty/c_\infty<1 \\[4mm] \dfrac{2A_\infty}{k}\displaystyle\int_{-\infty}^{x} V_\parallel(y)\sin\{k(x-y)\}dy & \text{when} \quad v_\infty/c_\infty>1, \end{cases} \tag{45}$$

where $k=2|v_\infty^2-c_\infty^2|^{1/2}$.

Denoting by σ the typical range of the potential $V_\parallel$, in the limit $k\sigma\gg1$ the Green function of Eq. (44) is almost a δ peak and Eqs. (45) take the simple form

$$\delta A(x)=\text{sgn}(v_\infty/c_\infty-1)\frac{2A_\infty}{k^2}V_\parallel(x). \tag{46}$$

This result may seem unnatural at large velocities. Indeed, for a repulsive potential, for instance, the density *increases* in the region of the potential. This kind of behavior was already found in Ref. [31], where a very special potential was designed for which this phenomenon occurs at any $v_\infty/c_\infty>1$.

From Eq. (46) we see that similar motional dressed states exist for any potential in the limit of very large velocities (when $k\sigma\gg1$).

In the case $v_\infty/c_\infty>1$, an asymptotic evaluation of Eq. (45) yields far ahead of the obstacle (in the limit $kx\gg1$) an amplitude of the form

$$\delta A(x)=\frac{2A_\infty}{k}\text{Im}\{e^{ikx}\hat V_\parallel(k)\}+\frac{2A_\infty}{k^2}V_\parallel(x)+O\!\left(\frac{1}{k^3}\right), \tag{47}$$

where $\hat V_\parallel(k)=\int_{-\infty}^{+\infty}dx\exp(-ikx)V_\parallel(x)$ is the Fourier transform of $V_\parallel(x)$. This shows that, for $v_\infty/c_\infty>1$, Eq. (45) cor-

responds to a C solution. The fact that the upstream solution oscillates with a wave vector k corresponds to the stationarity condition $v_p(k) = -v_\infty$ (see the end of Sec. IV). The wake is characterized by a wavelength $2\pi/k$ that depends on the velocity of the beam (it decreases when $|v_\infty|$ increases). This is due to the particular form of the dispersion relation (22), and does not occur above the Landau critical velocity in liquid helium, for instance, where the location of the roton minimum fixes the wavelength of the wake [32].

When the beam velocity is lower than the speed of sound, for attractive (repulsive) potentials Eq. (45) describes a B_1 (D_1) solution. In the attractive case, for instance, the bump density measured with respect to the constant density n_∞ contains a number ΔN of atoms given by $\Delta N = \int_{-\infty}^{+\infty} \delta n(x) dx \approx -(4n_\infty/k^2)\int_{-\infty}^{+\infty} dx V_\parallel(x)$. This formula diverges when $v_\infty/c_\infty \to 1$ since $k \to 0$. In that limit, however, the perturbative treatment is not justified. Indeed, Eq. (45) gives a sensible result only if $|\delta A| \ll A_\infty$. Denoting by V_0 the typical value of the potential $V_\parallel$, this reads

$$V_0 \sigma/k \ll 1 \quad \text{when} \quad k\sigma \ll 1,$$

$$V_0/k^2 \ll 1 \quad \text{when} \quad k\sigma \gg 1. \tag{48}$$

These conditions are satisfied only if the beam velocity v_∞ and the sound velocity c_∞ are not too close.

From Eqs. (45) we see that for $v_\infty/c_\infty < 1$ the typical length scale of variation of δA is proportional to k^{-1}. If $|v_\infty|$ approaches $|c_\infty|$ from below, this length scale diverges and the spatial extension of δA increases indefinitely. In this case it is legitimate to approximate $V_\parallel$ by a δ function. Hence, we do not pursue the perturbative treatment any longer and turn now to the study of solutions in a δ-function-peak potential.

Consider a potential of the form $V_\parallel(x) = \lambda \delta(x)$ with λ positive or negative. A realistic $V_\parallel$ can be approximated by such a potential if its typical length scale σ is much lower than the healing length ξ. In this case the approximation is valid for any beam velocity. As discussed above, any potential $V_\parallel$ can be approximated by a δ function when v_∞ approaches c_∞, i.e., in the limit $k\sigma \ll 1$.

The allowed transmission modes of Eq. (17) when $V_\parallel$ is a δ-function potential are very simple. They are obtained by joining together the solutions of two straight guides (see Sec. IV), one downstream ($x < 0$), and the other upstream ($x > 0$), with the matching condition

$$A'(0^+) - A'(0^-) = 2\lambda A(0). \tag{49}$$

The integration constant E_{cl} of Eq. (18) changes discontinuously from the value E_{cl}^- for $x < 0$ to the value E_{cl}^+ for $x > 0$ ($E_{cl}^\pm = \frac{1}{2}[A'(0^\pm)]^2 + W(n(0))$). Using Eq. (49) these two values are related through $E_{cl}^+ = E_{cl}^- + \lambda A(0)[A'(0^-) + A'(0^+)]$.

Let us first consider the case $v_\infty/c_\infty > 1$. We know from Secs. V B and VI A that one should observe C solutions. One has in this case a constant downstream density $n_\infty = A_\infty^2$ and $E_{cl}^- = W(n_\infty)$. The matching condition imposes $E_{cl}^+ = E_{cl}^- + 2\lambda^2 n_\infty$ and $A'(0^+) = 2\lambda A_\infty$. In order to have a finite solution at $x = +\infty$ one should moreover satisfy $W(n_\infty) \leq E_{cl}^+$
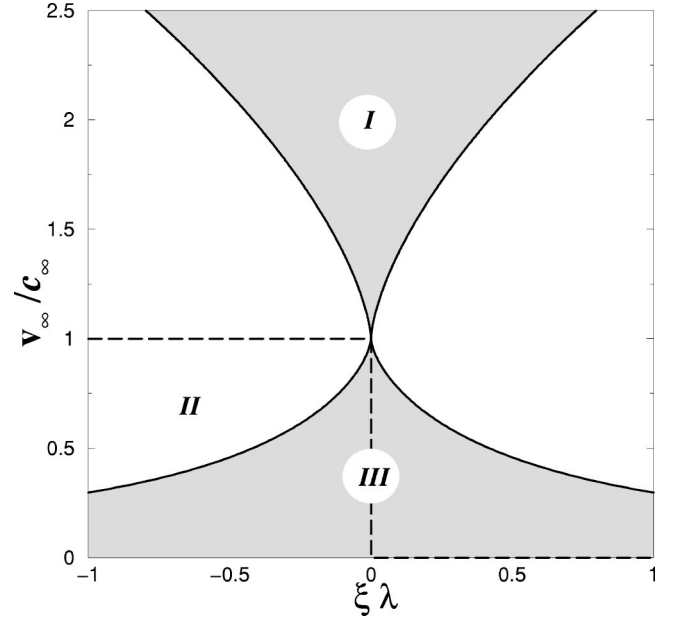

FIG. 13. Domains of existence of the different solutions occurring for a dilute beam in a potential $V_\parallel(x) = \lambda \delta(x)$. Region I occurs only for $v_\infty/c_\infty > 1$ and corresponds to C solutions. Region II corresponds to B_1 solutions and occupies the domain under the dashed line (it occurs only for attractive potentials and for $v_\infty/c_\infty < 1$). Region III corresponds to D solutions: D_1 solutions for $\lambda > 0$ and D_2 solutions when $\lambda < 0$.

$\leq W(n_2)$. This fixes an upper bound for the intensity of the perturbation, given by $2\lambda^2 n_\infty \leq W(n_2) - W(n_\infty)$. This is the criterion for observing C solutions. In the low-density limit this relation takes the analytical form

$$8\lambda^2 \xi^2 \leq F\left(\frac{v_\infty}{c_\infty}\right), \tag{50}$$

where the function F is defined in Eq. (34). It corresponds to the region I of Fig. 13.

Let us now consider the case $v_\infty/c_\infty < 1$. The first and simpler solution is the B_1 solution which occurs for attractive potentials. The corresponding matching condition (49) reads in this case $n'(0)/n(0) = -2\lambda$. It can be fulfilled whatever the value of λ ($\lambda < 0$) because the function $(n'/n)^2 = 8n^{-1}[E_{cl} - W(n)]$ can be made arbitrarily large [it grows as $8\varepsilon(n)/n$ for large n]. The domain of existence of B_1 solutions corresponds to region II in Fig. 13.

D solutions can also be observed if $v_\infty/c_\infty < 1$. For $\lambda > 0$ these are the D_1 solutions whose behavior in the $(n, W(n))$ diagram is illustrated in Fig. 12 (in the case of a depth of finite width though). For $\lambda < 0$ these are D_2 solutions such as those shown in Fig. 8 for $\sigma \to 0$. The limiting case (beyond which these solutions disappear) is obtained for two symmetric portions of solitary waves. The matching condition (49) then fixes the maximum value of $|\lambda|$, which corresponds in both cases to

$$|\lambda|\xi = K\left(\frac{v_\infty}{c_\infty}\right)$$

$$\text{where} \quad K(z) = \frac{1}{4z}\{-8z^4 - 20z^2 + 1 + (1+8z^2)^{3/2}\}^{1/2}. \tag{51}$$

The corresponding domain is shown in Fig. 13 (region III).

VIII. EXPERIMENTAL CONSIDERATIONS

In view of future experimental observation of the different flows past an obstacle, we now evaluate the orders of magnitude of the relevant dimensionless parameters identified above. For concreteness we consider a beam such as the one in preparation at the ENS [33]: ^{87}Rb atoms are guided along the x direction, with a harmonic transverse confinement ($\omega_\perp = 2\pi \times 500$ Hz and $a_\perp = 0.5$ μm). The beam has a velocity v_∞ of the order of 0.5 m/s and a flux Φ varying from 10^4 to 10^8 at. s^{-1}. Hence the quantity $n_\infty a_{sc}$ varies from 10^{-4} to 1. For a rough estimate of the order of magnitude of the relevant parameters, we will consider that this corresponds to the low-density limit $n_\infty a_{sc} \ll 1$. Then the healing length [defined in Eq. (9)] and the speed of sound vary from $\xi = 25$ μm and $c_\infty = 20$ μm s^{-1} (for $n_\infty a_{sc} = 10^{-4}$) to $\xi = 0.25$ μm and $c_\infty = 2$ mm s^{-1} ($n_\infty a_{sc} = 1$). Note that the beam velocity is much larger than the speed of sound (the quantity v_∞ / c_∞ is of order 10^3 at least).

If the obstacle is a bend of constant radius of curvature R_c and opening angle θ, $V_0 = -1/(8R_c^2)$ and $\sigma = \theta R_c$. A reasonable order of magnitude is $R_c = 5a_\perp$, leading to $V_0\xi^2 = \frac{1}{200}(\xi/a_\perp)^2$, which varies roughly from 10^{-3} to 10. For $\theta = \pi/2$ one has $\sigma = 8a_\perp$ and the obstacle can safely be treated perturbatively because in this case $k\sigma \sim 10^4 \gg 1$ and Eq. (48) is satisfied since

$$V_0/k^2 \approx 10^{-8} \ll 1.$$

For this configuration one thus expects profiles in agreement with Eq. (45) (case $v_\infty/c_\infty > 1$), i.e., C solutions. Also, since we are in the regime $k\sigma \gg 1$, Eq. (46) holds, meaning that the wake ahead of the obstacle is very weak, and that there is a decrease in the density in the region of the bend. However, this decrease is extremely small: it corresponds to a number of atoms smaller than unity, and under these conditions nothing noticeable is expected to occur in the bend.

The situation changes drastically if the obstacle is due to a transverse laser beam because the potential can be made much stronger. It can, moreover, be attractive or repulsive depending on the laser's frequency, and also the velocity of the obstacle relative to the beam can be modified by using an acousto-optic deflector.

We consider a laser with power $P = 70$ mW and a wavelength λ_L varying from 780 to 790 nm (the atomic transition corresponds to a wavelength $\lambda_A = 780.2$ nm and has a natural width $\Gamma = 12\pi$ MHz). The laser beam has a typical waist σ of the order of 50 μm. Then one obtains for the transverse potential

$$V_\parallel(x) = V_0 \exp\left\{-\frac{2x^2}{\sigma^2}\right\} \quad \text{where} \quad V_0 = \frac{\hbar\Gamma^2 P}{4\pi\delta\sigma^2 I_S}, \tag{52}$$

$\delta = \omega_A - \omega_L$ being the detuning and $I_S = 16$ W m^{-2} the saturation intensity. This yields

$$V_0\sigma^2 = \frac{1}{4\pi}\left(\frac{\Gamma^2}{\delta\omega_\perp}\right)\left(\frac{P}{I_S a_\perp^2}\right) \sim \pm 10^8. \tag{53}$$

In this case one is in the regime $k\sigma \gg 1$, with $V_0/k^2 \sim 10^{-2}$ or 10^{-1}. Hence one is on the edge of applicability of the perturbative approach. By changing the wavelength of the laser or its velocity with respect to the beam, one may enter into the nonperturbative regime. One can still find C solutions for this type of potential if the parameters of the system remain in the appropriate region of Fig. 10. C solutions exist for any value of σ if $V_0\xi^2 \leq \frac{1}{16}(v_\infty/c_\infty)^4$ in the case of an attractive potential, and if $V_0\xi^2 \leq \frac{1}{4}(v_\infty/c_\infty)^2$ in the case of a repulsive potential [since $v_\infty/c_\infty \gg 1$ we consider here the asymptotic versions of Eqs. (36) and (40)]. By modifying the value of the healing length and of the beam velocity these conditions can easily be satisfied or violated (especially in the case of repulsion). In the region where these conditions are violated one can experimentally study the transition from a stationary flow (of type C) to a time dependent one. For instance, it would be of great interest to study the modification of the drag at the transition.

Just at the boundary between the two regions, for a repulsive potential the density profile has the behavior shown in Fig. 11 [for an attractive potential the density profile corresponds to Fig. 9(b)]. The density has a steplike shape, and the beam ahead of the obstacle has a velocity lower than the speed of sound. One has just at the transition $\sigma = L_r$ (or L_a in the case of an attractive potential) with $8(V_0 L_r \xi)^2 \simeq F(v_\infty/c_\infty) \simeq (v_\infty/c_\infty)^4/4$ (see the end of Sec. VI A). From the estimate (53) this occurs for $\xi/\sigma \sim 10^{-2}$ or 10^{-3}. For a laser, one can tune the waist σ by a factor of order 5, say, and, more important, by changing the density one can modify the value of ξ and indeed reach the appropriate regime. This would have a very important effect on the beam, since the velocity ahead of the obstacle would be *lower* than the speed of sound whereas it is of the order of 1 m s^{-1} downstream. Accordingly, the density along the beam would go from $n_\infty = n_2$ to n_1 (see Fig. 11). It is not difficult to see that, in the dilute regime, in the limit $v_\infty/c_\infty \gg 1$ one has $n_2 \simeq n_1(v_\infty/c_\infty)^2/4$. Thus the downstream beam density is divided by a factor of order 10^6 with respect to the upstream one and, by conservation of the flux, the velocity is multiplied by the same factor. The beam velocity ahead of the obstacle is then of the order of a few micrometers per second.

IX. CONCLUSIONS

In this paper we have studied the different stationary profiles of a Bose-Einstein-condensed beam propagating through a guide with an obstacle. The beam far downstream is characterized by its velocity v_∞ and density n_∞ (or, equiva-

lently, its healing length ξ). The obstacle is represented by a one-dimensional square well of depth $\pm V_0$ and width σ. Let us denote by Δ the region along the guide where the potential is different from zero. Our study allows us to identify the relevant dimensionless parameters governing the flow across the obstacle. These are $n_\infty a_{sc}$, v_∞/c_∞, σ/ξ, and $V_0\xi^2$. By varying these parameters one obtains a wide range of density profiles (we identify three main stationary families denoted as B, C, and D solutions). We have numerically checked [34] that similar results are obtained for potentials other than square wells [such as $V_\parallel(x) = \pm V_0 \exp\{-x^2/\sigma^2\}$ for instance] and we thus believe that our analysis of the flow is quite general.

The richest case occurs when the external potential is attractive. In the subsonic regime (beam velocity lower than the corresponding speed of sound) the simplest solution is a symmetric density having a peak in Δ (B family). These solutions may have density oscillations in Δ, and are always symmetric. Another type of transmission mode is a soliton-like depressed solution pinned to the obstacle (D family), which may also have density oscillations in Δ and, unlike the B family, a wake upstream. Finally, the supersonic transmission modes (C solutions) possess, in the simplest case, a density trough in Δ and are constant outside. They may also have density oscillations in Δ and an upstream wake.

For a repulsive potential, in the subsonic regime the transmission modes are of type D with no density oscillations in Δ. In the supersonic case, the modes are of type C but with a density peak instead of a trough. Steplike solutions of increasing density across the obstacle (with or without wake) also exist. Specifically, we have identified an interesting (and experimentally reachable) regime where the beam is almost stopped by a repulsive obstacle and gains ahead of it several orders of magnitude in density (see Sec. VIII).

An important aspect of the problem that remains open are considerations related to the stability of the solutions. Some related work is in progress [34]. We just note here that the limiting C solution shown in Figs. 9(b) and 11 can be turned into a D solution by exchanging the downstream and the upstream behavior of the flow. However, these are part of a continuous family of flow patterns and are probably unstable. The C solutions, on the other hand, as selected by the radiation condition (see the end of Sec. IV), are the only acceptable ones for $v_\infty/c_\infty > 1$. Another aspect concerns Bose gases with attractive intra-atomic interactions, which may also be treated with our formalism. In this case the potential $W(n)$ introduced in Sec. IV has a single well shape, and the number of different transmission modes whose density tends to a constant at the input of the guide is greatly reduced with respect to the case of repulsive interactions considered here.

We conclude by noting that a branch of BEC that is now expanding is the nonlinear counterpart of transport experiments of mesoscopic physics in condensed matter. In the latter case the coherent transport of two-dimensional electron gases through various geometries has been considered in great detail. Future developments of transport experiments of Bose condensates should extend those to nonlinear regimes.

APPENDIX

In this Appendix we recall the conditions for existence of a bound state in a bend of an ordinary waveguide (i.e., without nonlinear terms in the Schrödinger equation) and put the adiabatic limit used in the text on firmer mathematical grounds.

Let us consider a curve $\mathcal{C}$, of parametric equation $\vec{r}_C(x)$, x being a curvilinear abscissa along $\mathcal{C}$. The Frenet frame $(\vec{t},\vec{n},\vec{b})$, the curvature $\kappa(x)$, and the torsion $\tau(x)$ are defined by $\vec{t}=d\vec{r}_C/dx$, $d\vec{t}/dx=\kappa\vec{n}$, $d\vec{n}/dx=-\kappa\vec{t}+\tau\vec{b}$, and $d\vec{b}/dx=-\tau\vec{n}$.

We first introduce a curvilinear coordinate system. The position of a point of space is specified by coordinates (x,y,z) through

$$\vec{r}(x,y,z)=\vec{r}_C(x)+y\vec{N}+z\vec{B}, \tag{A1}$$

where $\vec{N}(x)=\cos\theta\vec{n}+\sin\theta\vec{b}$, $\vec{B}(x)=-\sin\theta\vec{n}+\cos\theta\vec{b}$, and $\theta(x)$ is defined through $d\theta/dx=-\tau(x)$.

We then select a potential of the form $V_\perp(y,z)$. Note that the choice of vectors $\vec{N}$ and $\vec{B}$ for defining the transverse coordinates y and z is not irrelevant, i.e., the manner in which $V_\perp$ winds round $\mathcal{C}$ does matter: it has to be the same as the way $(\vec{N},\vec{B})$ winds around $\vec{t}$. Indeed, one can see that some torsion may create a repulsive potential along x, which could cancel the localizing effect of the bend. This is avoided with the type of coordinate dependence we have chosen. A simple way of seeing this is by noticing that $\vec{\nabla}$ has coordinates $(h^{-1}\partial_x,\partial_y,\partial_z)$ in the $(\vec{t},\vec{N},\vec{B})$ frame [with $h(x,y,z)=1-\kappa(y\cos\theta-z\cos\theta)$] and the force $-\vec{\nabla}V_\perp(y,z)$ thus has no tangential component. It would have been more natural to define the (y,z) coordinates as in Eq. (A1) but using the $(\vec{n},\vec{b})$ vectors instead of $(\vec{N},\vec{B})$. In this case, however, the force $-\vec{\nabla}V_\perp(y,z)$ would generically have a tangential component, which could spoil the localizing properties of the bend. Note that the latter discussion is of course irrelevant for a potential $V_\perp$ with circular symmetry (as any simple experimental wave guide is expected to have).

Denoting $h'=\partial_x h$ and $h''=\partial_{xx}^2 h$, the Schrödinger equation for $\Phi=h^{1/2}\Psi$ reads

$$-\frac{1}{2}\left(\frac{1}{h^2}\partial_{xx}^2+\partial_{yy}^2+\partial_{zz}^2\right)\Phi+\frac{h'}{h^3}\partial_x\Phi+\left[-\frac{\kappa^2}{8h^2}-\frac{5(h')^2}{8h^4}\right.$$

$$\left.+\frac{h''}{4h^3}+V_\perp(y,z)\right]\Phi=\mu\Phi. \tag{A2}$$

Note that in Eq. (A2), as in the rest of the paper, we take $\hbar = m = 1$. The choice of coordinates (A1) gives a volume element $d^3r = h\,dx\,dy\,dz$ and Φ is thus normalized as $\int dx\,dy\,dz\,|\Phi|^2 = 1$.

The adiabatic limit is defined by $h \to 1$, $\kappa \gg h'$, $\kappa \gg \sqrt{h''}$. In this limit Eq. (A2) decouples into a longitudinal and a transverse equation. One obtains for the longitudinal equation a potential $V_\parallel(x) = -\kappa^2(x)/8$, attractive in the region of the bend. Since any attractive potential in one dimension has a bound state [22], in this limit there exists a quantum state localized in the bend.

The theorem of Goldstone and Jaffe [19] establishes the existence of a bound state for much more general waveguides, with arbitrary curvature. It was originally demonstrated for sharp-wall waveguides, but the proof can be straightforwardly extended to the case of a smooth confining potential. Hence we do not reproduce its derivation here. We just note that for some points of space, the coordinate system (A1) can be ambiguous. This imposes for the sharp-wall problem the requirement that the transverse size of the guide does not exceed the radius of curvature of $\mathcal{C}$. For the smooth potential problem, the same restriction requires that the typical range of $V_\perp$ (or equivalently the spatial extension of $\phi_\perp$) is lower than the radius of curvature of $\mathcal{C}$. Obviously this condition is much weaker than the condition of adiabaticity. Note also that the Goldstone-Jaffe theorem has the same limitation as above, namely, some torsion may destroy the localizing effect of the bend and the way $V_\perp$ winds around the curve $\mathcal{C}$ is not irrelevant. A potential $V_\perp(y,z)$ where the coordinates y and z are defined above [Eqs. (A1)] ensures the applicability of the theorem.

---

[1] J. Denschlag, D. Cassettari, and J. Schmiedmayer, Phys. Rev. Lett. **82**, 2014 (1999).

[2] N. H. Dekker *et al.*, Phys. Rev. Lett. **84**, 1124 (2000).

[3] M. Key *et al.*, Phys. Rev. Lett. **84**, 1371 (2000).

[4] D. Müller, E. A. Cornell, D. Z. Anderson, and E. R. I. Abraham, Phys. Rev. A **61**, 033411 (2000).

[5] M.-O. Mewes *et al.*, Phys. Rev. Lett. **78**, 582 (1997).

[6] B. P. Anderson and M. Kasevich, Science **282**, 1686 (1998).

[7] E. W. Hagley *et al.*, Science **283**, 1706 (1999).

[8] I. Bloch, T. W. Hänsch, and T. Esslinger, Phys. Rev. Lett. **82**, 3008 (1999); Nature (London) **403**, 166 (2000).

[9] I. Bloch *et al.*, Phys. Rev. Lett. **87**, 030401 (2001).

[10] E. Mandonnet *et al.*, Eur. Phys. J. D **10**, 9 (2000).

[11] A. D. Jackson, G. M. Kavoulakis, and C. J. Pethick, Phys. Rev. A **58**, 2417 (1998).

[12] F. Dalfovo, S. Giorgini, L. P. Pitaevskii, and S. Stringari, Rev. Mod. Phys. **71**, 463 (1999).

[13] M. Olshanii, Phys. Rev. Lett. **81**, 938 (1998).

[14] J. H. Thywissen *et al.*, Eur. Phys. J. D **7**, 361 (1999).

[15] D. S. Petrov, G. V. Shlyapnikov, and J. T. M. Walraven, Phys. Rev. Lett. **85**, 3745 (2000).

[16] V. Dunjko, V. Lorent, and M. Olshanii, e-print cond-mat/0103085.

[17] D. W. L. Sprung and Hua Wu, J. Appl. Phys. **71**, 515 (1992).

[18] F. Kassubek, C. A. Stafford, and H. Grabert, Phys. Rev. B **59**, 7560 (1999).

[19] J. Goldstone and R. L. Jaffe, Phys. Rev. B **45**, 14 100 (1992).

[20] H. Wu, D. W. L. Sprung, and J. Martorell, Phys. Rev. B **45**, 11 960 (1992).

[21] J. T. Londergan, J. P. Carini, and D. P. Murdock, *Binding and Scattering in Two-Dimensional Systems* (Springer-Verlag, Berlin, 1999).

[22] L. Landau and E. M. Lifchitz, *Mécanique Quantique* (Éditions Mir, Moscow, 1988).

[23] Careful derivation shows that Eq. (13) is applicable for $N = 0$ in the limit $\sigma^{-2} \gg V_0$, where V_0 and σ are typical orders of magnitude for the depth and range of $V_\parallel(x)$, respectively. This condition corresponds to shallow potentials with a zero point energy much larger than V_0. If this condition is fulfilled for $N = 0$, increasing N increases the spatial extension of the bound state and makes the approximation even better justified. When N tends to N_{max} the approximation is valid for any type of potential (not necessarily shallow).

[24] E. Zaremba, Phys. Rev. A **57**, 518 (1998).

[25] S. Stringari, Phys. Rev. A **58**, 2385 (1998).

[26] P. O. Fedichev and G. V. Shlyapnikov, Phys. Rev. A **63**, 045601 (2001).

[27] G. B. Whitham, *Linear and Nonlinear Waves* (John Wiley, New York, 1974).

[28] H. Lamb, *Hydrodynamics* (Cambridge University Press, Cambridge, 1997).

[29] As discussed at the end of Sec. II, such bendings have been treated successfully for linear waves in Ref. [17] with an adiabatic approximation of the type (1).

[30] V. Hakim, Phys. Rev. E **55**, 2835 (1997).

[31] C. K. Law, C. M. Chan, P. T. Leung, and M.-C. Chu, Phys. Rev. Lett. **85**, 1598 (2000).

[32] L. P. Pitaevskii, JETP Lett. **39**, 423 (1984).

[33] D. Guéry-Odelin (private communication).

[34] P. Leboeuf and N. Pavloff (unpublished).